of patients (1). osteosarcoma originating in the pelvis and spine generally has a poor outcome. The prognosis of osteosarcoma patients older than 40 years is generally poor, probably because of their lower tolerance to high-dose chemotherapy and higher rate of axial tumor origin (1, 4). Through various experimental and assumption-based approaches, P-glycoprotein (multidrug resistance-1; ref. 5), ezrin (6), vascular endothelial growth factor (7, 8), matrix metalloproteinases (MMP; ref. 9), chemokine CXC motif receptor-4 (10), and other molecules have been shown to correlate significantly with outcome in osteosarcoma patients (11), but the clinical significance of these molecular biomarkers has not been established, and the molecular mechanisms behind the aggressive behavior of osteosarcoma still remain obscure.

Recently, Man and colleagues performed a microarray analysis of 34 cases of pediatric osteosarcoma and identified gene expression profiles that can predict response to chemotherapy (12). To clarify the alterations in gene expression associated with pulmonary metastasis, we have carefully selected cases with similar clinicopathologic backgrounds but demonstrating distinctly different outcomes, and did a microarray analysis under the assumption that osteosarcoma developing in older patients and/or in the trunk may have a different genetic background and different molecular mechanisms of progression. Here, we report that reduced expression of argininosuccinate synthetase (ASS) is a novel predictive biomarker for osteosarcoma patients with an unfavorable prognosis. Experimentally, osteosarcoma cells lacking ASS expression showed high sensitivity to arginine depletion. Our data seem to suggest a new therapeutic option for osteosarcoma patients with an unfavorable prognosis.

Materials and Methods

Patients and Tumor Samples

All tumor samples in this study were obtained by diagnostic incisional biopsy from primary sites of osteosarcoma before neoadjuvant chemotherapy at the National Cancer Center Hospital (Tokyo, Japan) between March 1996 and September 2007. We did not include patients older than 40 y and have primary tumors located outside the extremities. Each fresh tumor sample was cut into two pieces, one of which was immediately cryopreserved in liquid nitrogen, and the other fixed with formalin. The diagnosis of osteosarcoma and histologic subtypes were determined by certified pathologists. Only osteosarcoma samples with the osteoblastic, chondroblastic, fibroblastic, and telangiectatic histologic subtypes were included. The response to chemotherapy was classified as good if the extent of tumor necrosis was 90% or greater.

All patients provided written informed consent authorizing the collection and use of their samples for research purposes. The study protocol for obtaining clinical information and collecting samples was approved by the Institutional Review Board of the National Cancer Center (Tokyo, Japan).

Microarray Analysis

Total RNA was isolated using the IsoGen lysis buffer (Nippon Gene) and purified with a RNeasy Mini kit (Qiagen) in accordance with the manufacturer's protocol. We used a GeneChip Human Genome U133 Plus 2.0 array (Affymetrix) containing 54,613 probe sets. Target cRNA preparation, hybridization to the microarray, washing, staining, and scanning were done in accordance with the manufacturer's instructions (13). The relative expression values of the probe sets were calculated using the Array Assist 5.0 software package (Stratagene).

Real-time Reverse Transcription-PCR

For cDNA synthesis, 1 μg of total RNA was reverse transcribed by random priming with a High Capacity cDNA Reverse Transcription kit (Applied Biosystems). Gene-specific Taqman primers and probes were designed by Applied Biosystems. Amplification data measured as an increase in reporter fluorescence were collected using the PRISM 7000 Sequence Detection system (Applied Biosystems). The mRNA expression level relative to the internal control (*ACTB*, β-actin gene) was calculated by the comparative threshold cycle (C_T) method (14).

Immunohistochemistry

Human anti-ASS monoclonal antibody was purchased from BD Bioscience. Formalin-fixed, paraffin-embedded tissue sections (4 μm thick) were stained using a DAKO streptavidin-avidin-biotin complex kit (DAKO Corp.; ref. 15).

Cell Lines

The human osteosarcoma cell lines U-2, MNNG/HOS, and MG-63 were purchased from the American Tissue Culture Collection. NOS-1 and HuO-9N2 were purchased from Riken BRC Cell Bank. Arginine-containing and arginine-free media were prepared by the Cell Science & Technology Institute (Miyagi, Japan) and were supplemented with 10% dialyzed fetal bovine serum (Invitrogen).

A plasmid containing human ASS cDNA (pAS4/1/9) was obtained from the American Tissue Culture Collection. The ASS cDNA was subcloned into the EcoRV site of pcDNA3.1 (Invitrogen). Colony formation assay was done as previously described (16), and the areas occupied by colonies were quantified using the Image J software package (v1.41, NIH).

Western Blot Analysis

Anti–β-actin mouse monoclonal antibody (AC-74) was purchased from Sigma-Aldrich. Protein samples were subjected to SDS- PAGE and transferred to Immobilon-P membranes (Millipore). After an overnight incubation with primary antibodies at 4°C and with relevant secondary antibodies at room temperature for 1 h, blots were detected using enhanced chemiluminescence Western blotting detection reagents (GE Healthcare UK; ref. 17).

Table 1. Clinicopathologic characteristics of osteosarcoma patients analyzed using microarrays

Development of plumonary recurrence	Present (n = 7)	Abscent (n = 12)	
Gender			0.938*
Male	5	7	
Female	2	5	
Age			0.233
Mean (SD)	16 (5.3)	14 (4.0)	
Site of origin			0.317*
Femur, proximal	1	1	
Femur, distal	3	5	
Tibia, proximal	2	3	
Tibia, distal	1	2	
Other	0	1	
Histologic subtype			0.976*
Osteoblastic	6	9	
Others	1	3	
Metastasis at diagnosis			0.976*
Absent	6	9	
Present	1	3	
Neoajuvant chcemotherapy regimen			0.347
MTX+DOX/CDDP	5	5	
IFO+DOX/CDDP	2	5	
Others	0	2	
Response to neoadjuvant chemotherapy			0.667*
Good (necrosis ≥90%)	2	6	
Poor (necrosis <90%)	5	6	
Duration to the development of pulmonary metastasis (mo)			
Mean (SD)	28 (11.6)	NA	
Disease status			<0.001*
CDF	0	9	
NED	3	1	
DOD	4	2	
Follow-up period (mo)			0.290
Mean (SD), mo	62 (29.0)	72 (31.0)	
mRNA expression (microarray-based arbitrary unit), mean (SD)			
VEGF	1,151 (661)	2,519 (1,709)	0.056
MMP2	2,645 (1,812)	3,019 (2,158)	0.837
MMP9	6,521 (5,284)	7,981 (6,199)	0.711
CXCR4	989 (300)	844 (456)	0.536
TP53	108 (50)	74 (39)	0.120
ABCB1 (MDR1)	42 (10)	36 (5)	0.167
ERBB2 (Her2)	199 (96)	215 (69)	0.331
BIRC5 (Survivin)	424 (216)	432 (163)	0.711
VIL2 (Ezrin)	574 (213)	598 (321)	0.837
WT1	45 (9.0)	42 (5.9)	0.612
LRP5	48 (11)	51 (12)	0.482
FAS	303 (266)	316 (322)	0.837
ASS	86 (41)	541 (379)	<0.001

NOTE: Wilcoxon test was applied to assess differences in values.
Abbreviations: MTX, methotrexate; DOX, doxorubicin; CDDP, cisplatin; IFO ifosfamideof disease; NA, not applicable; CDF, chronic disease free; NED, no evidence of disease; DOD, deed of disease.
*Calculated by χ^2 test.

Fluorescence-Activated Cell Sorting

Cells were harvested using trypsinization and centrifuged at 1,000 rpm for 5 min. A CycleTEST PLUS DNA Reagent kit (Becton Dickinson) was used to stain the cells. DNA content was analyzed using a cell sorter (FACSCalibur, Becton Dickinson).

Statistical Analysis

Estimates of overall and metastasis-free survival were computed using the Kaplan-Meier method. Overall survival was calculated from the day of diagnosis until the end of follow-up or death. Metastasis-free survival was calculated from the day of diagnosis until the detection

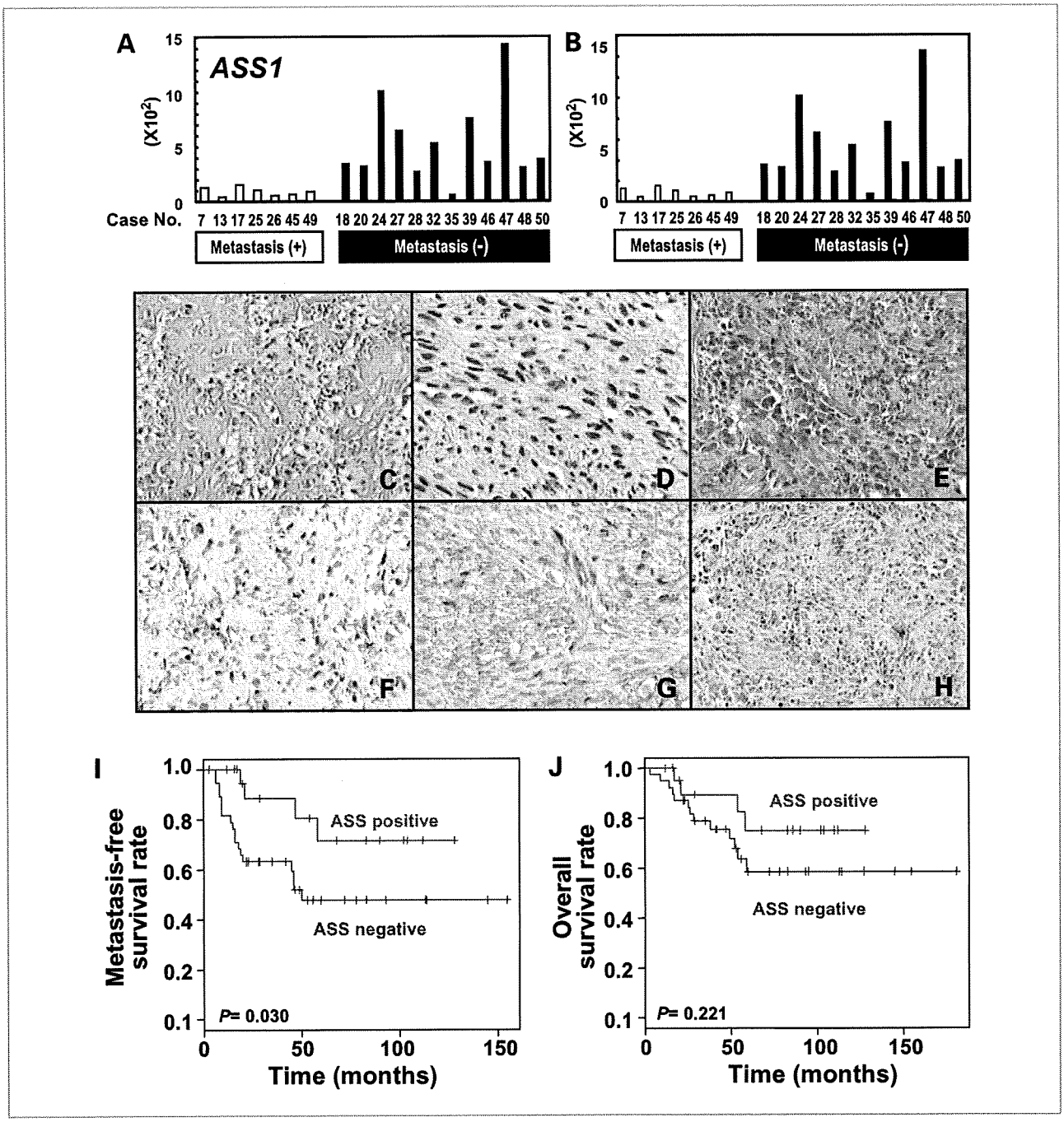

Figure 1. Downregulation of ASS in osteosarcoma patients who developed pulmonary metastasis. A and B, relative expression of ASS mRNA in osteosarcoma patients who did [metastasis (+)] and did not [metastasis (–)] develop pulmonary metastasis, determined by microarray and quantitative real-time reverse transcription-PCR (B). C to H, H&E (C–E) and immunoperoxidase (F–H) staining of ASS-positive (C, D, F, and G) and ASS-negative (E and H) osteosarcoma. I and J, Kaplan-Meier analysis of metastasis-free survival (I) and overall survival (J) of patients with ASS-positive and ASS-negative osteosarcoma.

Table 2. Clinicopathologic data of 62 osteosarcoma patients examined by immunohistochemistry

Variables	No. of patients	%
All	62	100
Gender		
Male	41	66
Female	21	34
Age		
<10	7	11
10–19	37	60
20–29	12	19
30–39	6	10
Location		
Lower extremity	55	89
Upper extremity	7	11
Histogical subtype		
Osteoblastic	35	56
Chondroblastic	10	16
Fibroblastic	3	5
Telangiectatic	3	5
Not determined	11	18
Metastasis at diagnosis		
Absent	53	85
Present	9	15
Response to neoadjuvant chemotherapy		
Good	21	34
Poor	35	56
NA	6	10
Development of pulmonary recurrence		
Yes	23	37
No	39	63
ASS protein expression		
Positive	22	35
Negative	39	63
Not evaluable	1	2

Abbreviation: NA, not available.

of new pulmonary lesions. Analyses such as the log-rank test, χ^2 test, and Cox proportional hazards regression model were done using the R statistical package version 2.7.0.[7] Differences at $P < 0.05$ were considered significant.

Results

Downregulation of ASS in Osteosarcoma Patients Developing Pulmonary Metastasis

We compared the gene expression profiles of biopsy samples obtained from 7 osteosarcoma patients who later developed lung metastasis within 4 years after neoadjuvant chemotherapy and subsequent surgical resection, and 12 patients who did not. The latter included three patients who had lung metastases at the time of diagnosis but did not relapse after lung resection. We carefully matched the distribution of gender, age, primary sites, histologic subtypes, and chemotherapeutic regimens between the two groups (Table 1). All of the 19 patients were <40 years of age and the biopsy samples were obtained from their primary lesions (not recurrent or metastatic tumors) in the upper or lower extremities before chemotherapy.

Genes that are reportedly correlated with the prognosis or metastasis of osteosarcoma, such as *VEGF* (7, 8), *MMP2/9* (9), *CXCR4* (10), *TP53* (18), *ABCB1* (5), *ERBB2* (19), *BIRC5* (20), *VIL2* (6), *WT1* (21), *LRP5* (22), and *FAS* (23), did not show significant differential expression (Table 1). Supplementary Tables S1 and S2 list 102 differentially expressed genes showing a fold change of >2.0 and a *P* value of <0.05. It is noteworthy that only 7 genes were upregulated in osteosarcoma patients who developed lung metastasis, whereas the remaining 95 genes were downregulated. Among these genes, *ASS* attracted our interest. The expression of *ASS* was downregulated 6.3-fold, with the highest statistical significance ($P = 2.2 \times 10^{-5}$), in osteosarcoma patients who developed lung metastasis (Supplementary Table S1; Fig. 1A). The microarray data were confirmed by real-time reverse transcription-PCR (Fig. 1B).

Validation by Immunohistochemistry

ASS protein expression was assessed immunohistochemically (Fig. 1C–H) in an independent cohort comprising 62 osteosarcoma patients (Table 2). The cohort included 41 males and 21 females. The average age at diagnosis was 18 years (7–38 years) and the mean follow-up period was 54 months (3–181 months). Of these 62 patients, 23 developed pulmonary metastasis during the study period. No patients developed metastasis in other organs without having a pulmonary lesion.

ASS expression was positive in 22 (Fig. 1F and G) and was negative in 39 specimens (Fig. 1H). Metastasis-free survival of patients with ASS-negative osteosarcoma was significantly worse than that of patients with ASS-positive osteosarcoma ($P = 0.030$, log-rank test; Fig. 1I). The estimated metastasis-free survival rate was 88.5% at 2 years and 71.5% at 5 years after treatment in ASS-positive patients, compared with 63.2% and 47.7%, respectively, in ASS-negative patients. There was no significant intergroup difference in overall survival ($P = 0.221$), but there was a trend of favorable survival probability for osteosarcoma with ASS expression (Fig. 1J). This was probably due to the relatively small cohort size. Cox regression analysis revealed that age, gender, primary tumor site (upper or lower extremity and proximal or distal location), histologic subtype, response to chemotherapy, and presence of metastasis at diagnosis were not significantly correlated with metastasis-free survival

[7] http://www.r-project.org/

Table 3. Univariate Cox regression analysis of metastasis-free survival

Variable	Hazard ratio	95% confidence interval		Z value	P
		Lower	Upper		
Age (y)					
<10 or ≥10	1.92	0.448	8.21	0.878	0.380
<20 or ≥20	1.94	0.836	4.512	1.55	0.120
<30 or ≥30	1.59	0.471	5.356	0.746	0.460
Gender					
Male or female	0.433	0.160	1.173	−1.64	0.100
Original site					
Lower or upper	1.14	0.338	3.824	0.207	0.840
Proximal or distal	0.93	0.401	2.154	−0.171	0.860
Histologic subtype					
Osteoblastic or others	1.240	0.450	3.423	0.416	0.680
Response to neoadjuvant chemotherapy					
Poor or good	0.627	0.24	1.638	−0.954	0.340
Metastasis at diagnosis					
Abscent or present	0.657	0.153	2.813	−0.565	0.570
ASS protein expression					
Negative or positive	0.319	0.108	0.945	−2.06	0.039*

*P value of < 0.05 was considered significant.

(Table 3). Only ASS expression was significantly correlated with metastasis-free survival ($P = 0.039$).

Overexpression of ASS Causes Growth Suppression of Osteosarcoma Cells

To examine the functional effect of ASS downregulation on osteosarcoma cell proliferation, four osteosarcoma cell lines (U2, NOS-1, MNNG/HOS, and MG63) were transfected with an expression plasmid containing human ASS cDNA (pcDNA3.1/ASS) or a control empty vector (pcDNA3.1). For all the cell lines, those transfected with pcDNA3.1/ASS formed significantly fewer colonies than those transfected with pcDNA3.1 (Fig. 2), indicating a growth-suppressive effect of ASS on osteosarcoma cells.

Cell Growth Inhibition of Osteosarcoma Showing Low ASS Expression Due to Arginine Deprivation

ASS is an essential enzyme for the production of arginine. U2 cells, which express a high amount of ASS (Fig. 3A), grew equally well in arginine-containing and arginine-free medium. Fluorescence-activated cell sorting analysis of U2 cells revealed no significant difference between those cultured in arginine-containing medium and those grown in arginine-free medium. On the other hand, the four cell lines with relatively low ASS expression (MNNG/HOS, NOS-1, HuO9N2, and MG63; Fig. 3A) showed no cell growth at all when cultured with arginine-free medium (Fig. 3B). An increase in the proportion of cells in the G_1 phase and a decrease of those in the G_2-M phase were observed in the four cell lines with relatively low ASS expression when the cells were cultured in arginine-free medium (Fig. 3C). These results indicated that arginine deprivation induced G_1 arrest in osteosarcoma cells with low ASS expression.

Discussion

Control of pulmonary metastasis is essential for improving the prognosis of osteosarcoma, and there is an urgent need to clarify the molecular mechanisms behind the process of metastasis, which could lead to the discovery of novel therapeutic approaches for osteosarcoma. Although several molecules associated with the metastatic potential of osteosarcoma have been identified by assumption- and microarray-based analyses, the lack of consistent results in reports to date precludes any definitive assessment of those molecules (11). This is likely due to the limited number of osteosarcoma patients as well as their heterogeneous characteristics such as age, tumor site, histologic subtype, and treatment history before sample collection. To identify more accurate predictive markers for patients at high risk of lung metastasis, appropriate patient selection is vital. We therefore assessed the expression profiles of a cohort of osteosarcoma patients ages <40 years whose tumors were located in the limbs (Table 1). The specimens were obtained by diagnostic biopsy from the primary sites of osteosarcoma to unify the sample conditions, and this sample cohort was composed of all four major histologic subtypes of osteosarcoma to minimize any selection bias. Our microarray

analysis revealed that expression of ASS was significantly downregulated in osteosarcoma patients with postoperative metastasis (Fig. 1A and B). Moreover, we found a remarkable correlation between ASS expression and metastasis-free survival in osteosarcoma patients (Table 3), indicating that the loss of ASS could serve as a predictive biomarker for the postsurgical pulmonary recurrence of osteosarcoma. The expression of various genes has been reported to correlate with the outcome of osteosarcoma patients, but none of these showed a significant correlation with the development of pulmonary metastasis in our microarray analysis (Table 1), probably because of the different criteria used for the selection of cases for the analysis. However, four ASS-positive patients in the validation cohort developed pulmonary metastases (Fig. 1I), indicating that some unknown factor(s) other than ASS is also involved in the process of pulmonary metastasis.

ASS is a rate-limiting enzyme in the biosynthesis of arginine, converting citrulline to argininosuccinate, the immediate precursor of arginine (24, 25). ASS has three major functions in mammalian organisms: (*a*) ammonia detoxication through the urea cycle in the liver, (*b*) arginine production in the kidney proximal tubule, and (*c*) arginine synthesis for the production of nitric oxide in various cells (24, 25). Previous studies by others have shown that ASS deficiency is frequently evident in several human cancers, including melanoma, hapatocellular

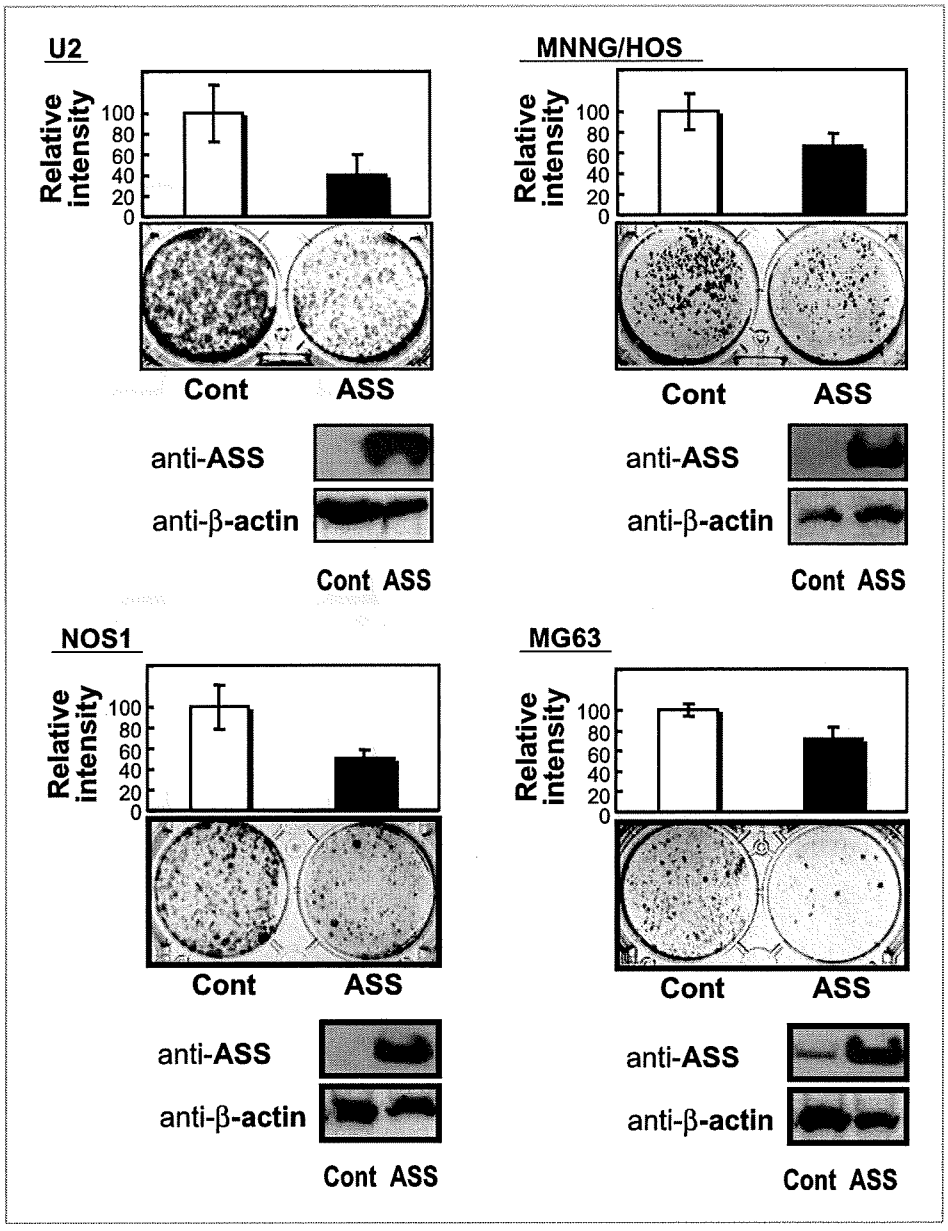

Figure 2. Effects of ASS expression on osteosarcoma cell growth. Colony formation of four osteosarcoma cell lines transfected with empty pcDNA3.1 vector (cont) and pcDNA3.1/ASS (ASS). Transfectants were cultured in the presence of G418 for 10 d, and then stained. Two days after transfection, cell lysates were subjected to immunoblotting with antibodies against ASS and β-actin (loading control).

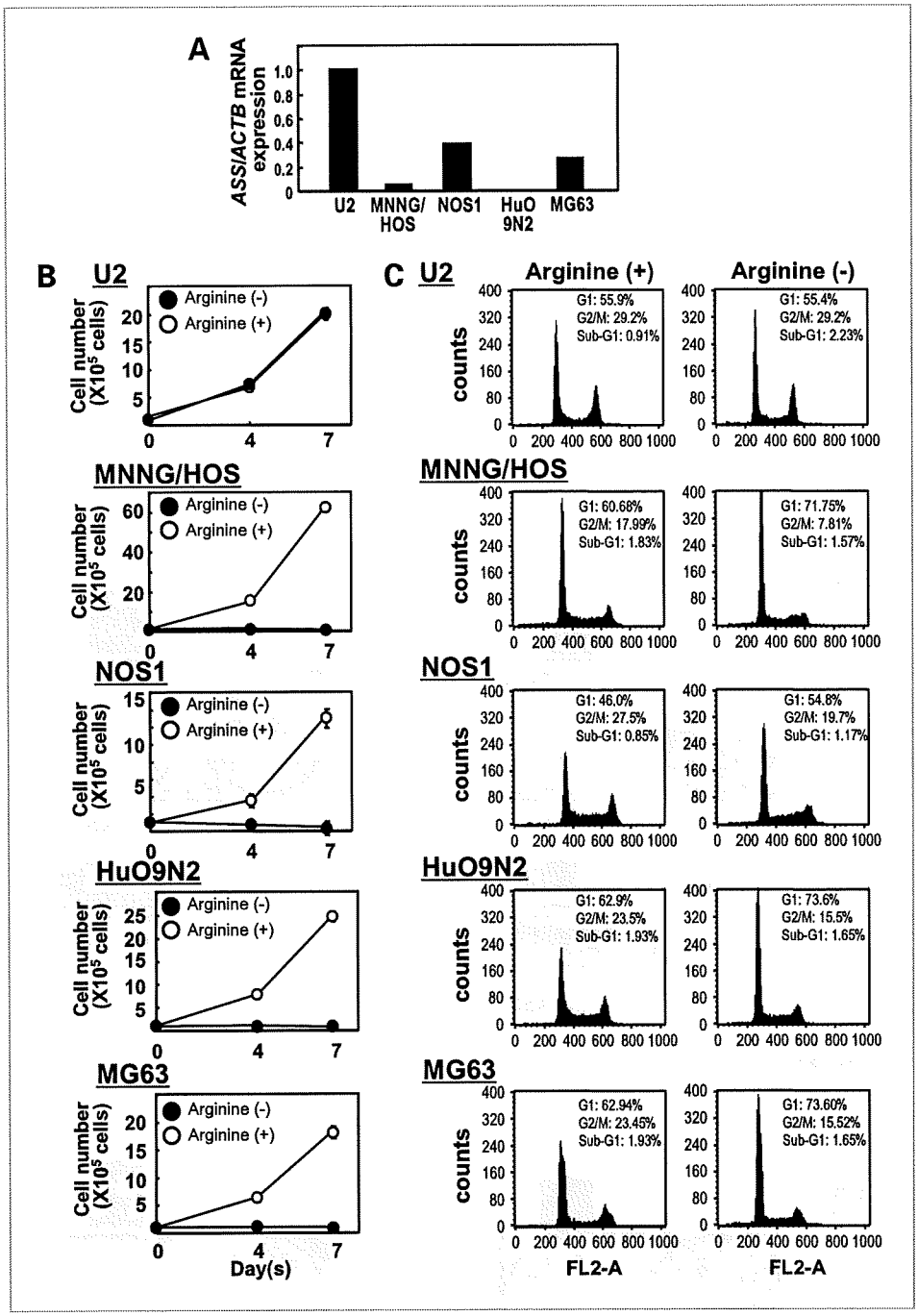

Figure 3. Effect of arginine deprivation on growth of osteosarcoma cells. A, relative *ASS* mRNA expression of five osteosarcoma cell lines determined by real-time reverse transcription-PCR. B, osteosarcoma cells were plated at 1.0×10^5 per well into six-well microplates and cultured in arginine-containing [arginine (+)] or arginine-free [arginine (–)] medium. The numbers of cells were then counted by trypan blue dye exclusion using a hemocytometer. C, osteosarcoma cells were cultured in arginine-containing (left) or arginine-free (right) medium for 3 d, and subjected to cell sorter analysis. The percentages of cells in the sub-G_1, G_1, and G_2-M phase are indicated.

carcinoma (HCC), and prostate carcinoma (26), and ASS deficiency is significantly associated with the lymphatic dissemination of esophageal carcinoma (27). However, no studies have clarified the mechanisms by which lack of ASS confers malignant phenotypes on tumor cells or how the *ASS* gene is downregulated. In the present study, we showed that the restoration of ASS expression in osteosarcoma cell lines suppressed their growth (Fig. 2). Considering that the lack of ASS expression is frequently observed in cells of several other cancers, such as melanoma and HCC, ASS may regulate normal cellular functions, thereby working as a tumor suppressor. Alternatively, the gain of arginine from the microenvironment or the circulation might confer some growth advantage on ASS-negative tumor cells, instead of generating arginine on their own. Further work is needed to clarify the role of ASS in the inhibition of tumor cell growth. In an attempt to investigate the molecular mechanism

of *ASS* gene silencing, we tried to restore ASS expression by treating the osteosarcoma cells with a methyltransferase inhibitor, 5-aza-2′-deoxycytidine. However, we observed no effects on the restoration of ASS in these cells, indicating that the promoter methylation of the *ASS* gene is not responsible for the silencing of ASS (data not shown).

Because tumors not expressing ASS are auxotrophic for arginine, arginine deprivation has been reported to be an effective anticancer treatment for ASS-deficient tumors, as exemplified by HCC, melanoma, and renal cell carcinoma, both *in vitro* and *in vivo*, and also by malignant mesothelioma, retinoblastoma, and pancreatic cancer *in vitro* (28–36). It is therefore plausible that ASS deficiency could become a therapeutic target for osteosarcoma, besides being a predictive biomarker for postsurgical pulmonary metastasis. The effect of arginine deprivation has not been established in osteosarcoma (37). We showed that four osteosarcoma cell lines with low levels of ASS expression failed to grow in arginine-free medium, whereas ASS-positive cells were able to grow in medium with or without arginine. Furthermore, osteosarcoma cells that did not proliferate in arginine-free medium underwent G_0-G_1 arrest (Fig. 3B and C). In such cells, the sub–G_0-G_1 population was barely detectable, indicating that arginine deprivation for 3 days did not cause apoptosis. This finding may not contradict a previous observation by Gong et al. (37), who showed that arginine deiminase (ADI) induced apoptosis in cultured cells only at high concentration. ADI seems to have a variety of pharmacologic activities besides arginine depletion (31, 37–41).

Based on our present findings, we propose a new therapeutic approach for the management of osteosarcoma patients who are at high risk of lung metastasis. Before starting neoadjuvant chemotherapy, diagnostic biopsy specimens from osteosarcoma patients should be screened for ASS by immunohistochemical assay. Then, for those lacking ASS or expressing ASS at reduced levels, systemic arginine deprivation is recommended to reduce the risk of developing pulmonary metastasis. Given that ~50% of osteosarcoma patients are resistant to current chemotherapy, this approach could be a promising strategy for eradicating tumor cells in osteosarcoma patients with a higher recurrence potential, thus improving their prognosis. Encouraging results of arginine deprivation therapy with the use of ADI have recently been shown both *in vitro* and *in vivo* (28–30). Phase I and II trials of ADI-PEG20, a derivative of ADI with a prolonged half-life, have shown a partial response with tolerable adverse effects in patients with melanoma and HCC (34, 35). Future clinical trials are warranted to establish the clinical potential of systemic arginine deprivation therapy for osteosarcoma patients.

Our data indicate that ASS could serve as not only a novel predictive biomarker for metastasis development, but also become a potential target for pharmacologic intervention. Elucidation of the molecular mechanisms by which a reduced level of ASS increases the chances of pulmonary metastasis will be necessary.

Disclosure of Potential Conflicts of Interest

No potential conflicts of interest were disclosed.

Acknowledgments

We thank Dr. Kazutaka Kikuta (National Cancer Center Research Institute, Tokyo, Japan) for collecting the samples and Sachiyo Mitani and Yuka Nakmura for their technical assistance.

Grant Support

Program for Promotion of Fundamental Studies in Health Sciences conducted by the National Institute of Biomedical Innovation of Japan (05-30) and the Third-Term Comprehensive Control Research for Cancer and Research on Biological Markers for New Drug Development conducted by the Ministry of Health, Labor, and Welfare of Japan. E. Kobayashi is the Awardee of a Research Resident Fellowship from the Foundation for Promotion of Cancer Research (Tokyo, Japan) for the Third Term Comprehensive 10-Year Strategy for Cancer Control.

The costs of publication of this article were defrayed in part by the payment of page charges. This article must therefore be hereby marked *advertisement* in accordance with 18 U.S.C. Section 1734 solely to indicate this fact.

Received 08/19/2009; revised 12/03/2009; accepted 12/15/2009; published OnlineFirst 02/16/2010.

References

1. Bielack SS, Kempf-Bielack B, Delling G, et al. Prognostic factors in high-grade osteosarcoma of the extremities or trunk: an analysis of 1,702 patients treated on neoadjuvant cooperative osteosarcoma study group protocols. J Clin Oncol 2002;20:776–90.
2. Meyers PA, Gorlick R, Heller G, et al. Intensification of preoperative chemotherapy for osteogenic sarcoma: results of the Memorial Sloan-Kettering (T12) protocol. J Clin Oncol 1998;16:2452–8.
3. Ferguson WS, Goorin AM. Current treatment of osteosarcoma. Cancer Invest 2001;19:292–315.
4. Carsi B, Rock MG. Primary osteosarcoma in adults older than 40 years. Clin Orthop 2002:53–61.
5. Baldini N, Scotlandi K, Barbanti-Brodano G, et al. Expression of P-glycoprotein in high-grade osteosarcomas in relation to clinical outcome. N Engl J Med 1995;333:1380–5.
6. Khanna C, Wan X, Bose S, et al. The membrane-cytoskeleton linker ezrin is necessary for osteosarcoma metastasis. Nat Med 2004;10:182–6.
7. Kaya M, Wada T, Akatsuka T, et al. Vascular endothelial growth factor expression in untreated osteosarcoma is predictive of pulmonary metastasis and poor prognosis. Clin Cancer Res 2000;6:572–7.
8. Tsunemi T, Nagoya S, Kaya M, et al. Postoperative progression of pulmonary metastasis in osteosarcoma. Clin Orthop 2003:159–66.
9. Foukas AF, Deshmukh NS, Grimer RJ, Mangham DC, Mangos EG, Taylor S. Stage-IIB osteosarcomas around the knee. A study of MMP-9 in surviving tumour cells. J Bone Joint Surg Br 2002;84:706–11.
10. Laverdiere C, Hoang BH, Yang R, et al. Messenger RNA expression levels of CXCR4 correlate with metastatic behavior and outcome in patients with osteosarcoma. Clin Cancer Res 2005;11:2561–7.
11. Clark JC, Dass CR, Choong PF. A review of clinical and molecular

prognostic factors in osteosarcoma. J Cancer Res Clin Oncol 2008; 134:281–97.
12. Man TK, Chintagumpala M, Visvanathan J, et al. Expression profiles of osteosarcoma that can predict response to chemotherapy. Cancer Res 2005;65:8142–50.
13. Yamaguchi U, Nakayama R, Honda K, et al. Distinct gene expression-defined classes of gastrointestinal stromal tumor. J Clin Oncol 2008;26:4100–8.
14. Huang L, Shitashige M, Satow R, et al. Functional interaction of DNA topoisomerase IIα with the β-catenin and T-cell factor-4 complex. Gastroenterology 2007;133:1569–78.
15. Nitori N, Ino Y, Nakanishi Y, et al. Prognostic significance of tissue factor in pancreatic ductal adenocarcinoma. Clin Cancer Res 2005; 11:2531–9.
16. Shitashige M, Satow R, Honda K, Ono M, Hirohashi S, Yamada T. Regulation of Wnt signaling by the nuclear pore complex. Gastroenterology 2008;134:1961–71, 71 e1–4.
17. Idogawa M, Masutani M, Shitashige M, et al. Ku70 and poly(ADP-ribose) polymerase-1 competitively regulate β-catenin and T-cell factor-4-mediated gene transactivation: possible linkage of DNA damage recognition and Wnt signaling. Cancer Res 2007;67:911–8.
18. Park YB, Kim HS, Oh JH, Lee SH. The co-expression of p53 protein and P-glycoprotein is correlated to a poor prognosis in osteosarcoma. Int Orthop 2001;24:307–10.
19. Zhou H, Randall RL, Brothman AR, Maxwell T, Coffin CM, Goldsby RE. Her-2/neu expression in osteosarcoma increases risk of lung metastasis and can be associated with gene amplification. J Pediatr Hematol Oncol 2003;25:27–32.
20. Osaka E, Suzuki T, Osaka S, et al. Survivin as a prognostic factor for osteosarcoma patients. Acta Histochem Cytochem 2006;39:95–100.
21. Srivastava A, Fuchs B, Zhang K, et al. High WT1 expression is associated with very poor survival of patients with osteogenic sarcoma metastasis. Clin Cancer Res 2006;12:4237–43.
22. Hoang BH, Kubo T, Healey JH, et al. Expression of LDL receptor-related protein 5 (LRP5) as a novel marker for disease progression in high-grade osteosarcoma. Int J Cancer 2004;109:106–11.
23. Lafleur EA, Koshkina NV, Stewart J, et al. Increased Fas expression reduces the metastatic potential of human osteosarcoma cells. Clin Cancer Res 2004;10:8114–9.
24. Wu G, Morris SM, Jr. Arginine metabolism: nitric oxide and beyond. Biochem J 1998;336:1–17.
25. Husson A, Brasse-Lagnel C, Fairand A, Renouf S, Lavoinne A. Argininosuccinate synthetase from the urea cycle to the citrulline-NO cycle. Eur J Biochem 2003;270:1887–99.
26. Dillon BJ, Prieto VG, Curley SA, et al. Incidence and distribution of argininosuccinate synthetase deficiency in human cancers: a method for identifying cancers sensitive to arginine deprivation. Cancer 2004; 100:826–33.
27. Lagarde SM, Ver Loren van Themaat PE, Moerland PD, et al. Analysis of gene expression identifies differentially expressed genes and pathways associated with lymphatic dissemination in patients with adenocarcinoma of the esophagus. Ann Surg Oncol 2008;15: 3459–70.
28. Ensor CM, Holtsberg FW, Bomalaski JS, Clark MA. Pegylated arginine deiminase (ADI-SS PEG20,000 mw) inhibits human melanomas and hepatocellular carcinomas *in vitro* and *in vivo*. Cancer Res 2002; 62:5443–50.
29. Wheatley DN, Campbell E. Arginine deprivation, growth inhibition and tumour cell death: 3. Deficient utilisation of citrulline by malignant cells. Br J Cancer 2003;89:573–6.
30. Yoon CY, Shim YJ, Kim EH, et al. Renal cell carcinoma does not express argininosuccinate synthetase and is highly sensitive to arginine deprivation via arginine deiminase. Int J Cancer 2007;120:897–905.
31. Szlosarek PW, Klabatsa A, Pallaska A, et al. *In vivo* loss of expression of argininosuccinate synthetase in malignant pleural mesothelioma is a biomarker for susceptibility to arginine depletion. Clin Cancer Res 2006;12:7126–31.
32. Bowles TL, Kim R, Galante J, et al. Pancreatic cancer cell lines deficient in argininosuccinate synthetase are sensitive to arginine deprivation by arginine deiminase. Int J Cancer 2008;123:1950–5.
33. Kim JH, Yu YS, Kim DH, Min BH, Kim KW. Anti-tumor activity of arginine deiminase via arginine deprivation in retinoblastoma. Oncol Rep 2007;18:1373–7.
34. Ascierto PA, Scala S, Castello G, et al. Pegylated arginine deiminase treatment of patients with metastatic melanoma: results from phase I and II studies. J Clin Oncol 2005;23:7660–8.
35. Izzo F, Marra P, Beneduce G, et al. Pegylated arginine deiminase treatment of patients with unresectable hepatocellular carcinoma: results from phase I/II studies. J Clin Oncol 2004;22:1815–22.
36. Shen LJ, Lin WC, Beloussow K, Shen WC. Resistance to the antiproliferative activity of recombinant arginine deiminase in cell culture correlates with the endogenous enzyme, argininosuccinate synthetase. Cancer Lett 2003;191:165–70.
37. Gong H, Zolzer F, von Recklinghausen G, et al. Arginine deiminase inhibits cell proliferation by arresting cell cycle and inducing apoptosis. Biochem Biophys Res Commun 1999;261:10–4.
38. Gong H, Zolzer F, von Recklinghausen G, Havers W, Schweigerer L. Arginine deiminase inhibits proliferation of human leukemia cells more potently than asparaginase by inducing cell cycle arrest and apoptosis. Leukemia 2000;14:826–9.
39. Beloussow K, Wang L, Wu J, Ann D, Shen WC. Recombinant arginine deiminase as a potential anti-angiogenic agent. Cancer Lett 2002;183:155–62.
40. Park IS, Kang SW, Shin YJ, et al. Arginine deiminase: a potential inhibitor of angiogenesis and tumour growth. Br J Cancer 2003;89: 907–14.
41. Gong H, Pottgen C, Stuben G, Havers W, Stuschke M, Schweigerer L. Arginine deiminase and other antiangiogenic agents inhibit unfavorable neuroblastoma growth: potentiation by irradiation. Int J Cancer 2003;106:723–8.

Supplementary Table S1. List of genes whose expression was significantly down-regulated in OS patients who developed pulmonary metastasis ($P < 0.05$)

Probe Set ID	Gene symbol	Description	*P*-value	Fold change
207076_s_at	ASS1	argininosuccinate synthetase 1	2.20E-05	6.305
218424_s_at	STEAP3	STEAP family member 3	0.00126	2.150
237452_at	---	Transcribed locus	0.00130	2.384
237773_at	---	Transcribed locus	0.00224	2.175
225863_s_at	C19orf12	chromosome 19 open reading frame 12	0.00272	2.025
201036_s_at	HADH	hydroxyacyl-Coenzyme A dehydrogenase	0.00299	2.003
219454_at	EGFL6	EGF-like-domain, multiple 6	0.00304	9.457
228844_at	SLC13A5	solute carrier family 13 (sodium-dependent citrate transporter), member 5	0.00321	2.117
229963_at	BEX5	BEX family member 5	0.00334	4.086
204223_at	PRELP	proline/arginine-rich end leucine-rich repeat protein	0.00342	4.340
205908_s_at	OMD	osteomodulin	0.00443	4.035
225293_at	COL27A1	collagen, type XXVII, alpha 1	0.00459	2.583
227655_at	---	CDNA FLJ38512 fis, clone HCHON2000503	0.00462	2.187
205907_s_at	OMD	osteomodulin	0.00473	3.602
225288_at	COL27A1	collagen, type XXVII, alpha 1	0.00548	2.842
223836_at	FGFBP2	fibroblast growth factor binding protein 2	0.00574	13.529
224020_at	MGC4473	hypothetical LOC79100	0.00580	3.149
223983_s_at	C19orf12	chromosome 19 open reading frame 12	0.00617	2.152
205679_x_at	ACAN	aggrecan	0.00641	5.251
210258_at	RGS13	regulator of G-protein signaling 13	0.00755	2.317
226760_at	LOC203411	hypothetical protein LOC203411	0.00975	2.120
207692_s_at	ACAN	aggrecan	0.01006	6.008
204400_at	EFS	embryonal Fyn-associated substrate	0.01043	2.041
202709_at	FMOD	fibromodulin	0.01068	6.475
228224_at	PRELP	proline/arginine-rich end leucine-rich repeat protein	0.01139	3.433
210367_s_at	PTGES	prostaglandin E synthase	0.01216	2.525
213492_at	COL2A1	collagen, type II, alpha 1	0.01341	21.271
210839_s_at	ENPP2	ectonucleotide pyrophosphatase/phosphodiesterase 2 (autotaxin)	0.01351	2.547
202575_at	CRABP2	cellular retinoic acid binding protein 2	0.01390	2.716
217161_x_at	ACAN	aggrecan	0.01398	4.895
202920_at	ANK2	ankyrin 2, neuronal	0.01425	2.990
209628_at	NXT2	nuclear transport factor 2-like export factor 2	0.01456	2.168
202219_at	SLC6A8	solute carrier family 6 (neurotransmitter transporter, creatine), member 8	0.01469	2.042
224345_x_at	C3orf28	chromosome 3 open reading frame 28	0.01484	2.349
206172_at	IL13RA2	interleukin 13 receptor, alpha 2	0.01508	5.689
209392_at	ENPP2	ectonucleotide pyrophosphatase/phosphodiesterase 2 (autotaxin)	0.01512	2.206
231131_at	FAM133A	family with sequence similarity 133, member A	0.01598	2.812
223193_x_at	C3orf28	chromosome 3 open reading frame 28	0.01612	2.331
221584_s_at	KCNMA1	potassium large conductance calcium-activated channel, subfamily M, alpha member 1	0.01629	2.209
217525_at	OLFML1	olfactomedin-like 1	0.01633	2.190
232267_at	GPR133	G protein-coupled receptor 133	0.01676	2.025
228218_at	---	CDNA clone IMAGE:5284125	0.01836	2.057
203570_at	LOXL1	lysyl oxidase-like 1	0.01860	2.524
204508_s_at	CA12	carbonic anhydrase XII	0.01922	2.591
211276_at	TCEAL2	transcription elongation factor A (SII)-like 2	0.01938	4.972
204736_s_at	CSPG4	chondroitin sulfate proteoglycan 4	0.01993	2.178
213348_at	CDKN1C	cyclin-dependent kinase inhibitor 1C (p57, Kip2)	0.02170	2.185
205475_at	SCRG1	scrapie responsive protein 1	0.02189	20.654
220942_x_at	C3orf28	chromosome 3 open reading frame 28	0.02291	2.178
39729_at	PRDX2	peroxiredoxin 2	0.02310	2.222
214164_x_at	CA12	carbonic anhydrase XII	0.02463	2.810
230204_at	---	Transcribed locus	0.02469	5.283
232010_at	FSTL5	follistatin-like 5	0.02477	3.505
210511_s_at	INHBA	inhibin, beta A	0.02595	2.179
239481_at	FAM133A	family with sequence similarity 133, member A	0.02598	3.027
201261_x_at	BGN	biglycan	0.02718	2.386
202868_s_at	POP4	processing of precursor 4, ribonuclease P/MRP subunit (S. cerevisiae)	0.02766	2.204
227240_at	NGEF	neuronal guanine nucleotide exchange factor	0.02795	2.773
210512_s_at	VEGFA	vascular endothelial growth factor A	0.02845	2.188
230372_at	HAS2	Hyaluronan synthase 2	0.03010	2.571
230895_at	---	Transcribed locus	0.03018	4.559

206432_at	HAS2	hyaluronan synthase 2	0.03090	2.436
223687_s_at	LY6K	lymphocyte antigen 6 complex, locus K	0.03109	2.927
204932_at	TNFRSF11B	tumor necrosis factor receptor superfamily, member 11b (osteoprotegerin	0.03150	2.819
202935_s_at	SOX9	SRY (sex determining region Y)-box 9 (campomelic dysplasia, autosomal sex-reversal)	0.03178	2.396
228214_at	---	Transcribed locus	0.03307	2.034
213905_x_at	BGN	biglycan	0.03345	2.434
218730_s_at	OGN	osteoglycin	0.03417	5.400
217404_s_at	COL2A1	collagen, type II, alpha 1	0.03422	19.284
205081_at	CRIP1	cysteine-rich protein 1 (intestinal)	0.03467	2.078
212171_x_at	VEGFA	vascular endothelial growth factor A	0.03535	2.031
210145_at	PLA2G4A	phospholipase A2, group IVA (cytosolic, calcium-dependent)	0.03538	2.277
214297_at	CSPG4	chondroitin sulfate proteoglycan 4	0.03705	2.212
222043_at	CLU	clusterin	0.03836	2.974
205523_at	HAPLN1	hyaluronan and proteoglycan link protein 1	0.03897	3.910
207177_at	PTGFR	prostaglandin F receptor (FP)	0.04037	2.926
209189_at	FOS	v-fos FBJ murine osteosarcoma viral oncogene homolog	0.04090	2.109
202410_x_at	IGF2 /// INS /// INS-IGF2	insulin-like growth factor 2 (somatomedin A) /// insulin /// INS-IGF2	0.04110	2.086
204724_s_at	COL9A3	collagen, type IX, alpha 3	0.04126	4.816
222722_at	OGN	osteoglycin	0.04157	4.682
203963_at	CA12	carbonic anhydrase XII	0.04177	2.506
227140_at	---	CDNA FLJ11041 fis, clone PLACE1004405	0.04272	2.160
215867_x_at	CA12	carbonic anhydrase XII	0.04364	2.506
209815_at	PTCH1	patched homolog 1 (Drosophila)	0.04393	2.823
229839_at	SCARA5	Scavenger receptor class A, member 5 (putative)	0.04394	2.219
204844_at	ENPEP	glutamyl aminopeptidase (aminopeptidase A)	0.04647	2.050
208651_x_at	CD24	CD24 molecule	0.04673	2.325
266_s_at	CD24	CD24 molecule	0.04677	2.731
218484_at	NDUFA4L2	NADH dehydrogenase (ubiquinone) 1 alpha subcomplex, 4-like 2	0.04732	3.466
227498_at	---	CDNA FLJ11723 fis, clone HEMBA1005314	0.04748	2.363
216379_x_at	CD24	CD24 molecule	0.04815	2.642
204933_s_at	TNFRSF11B	tumor necrosis factor receptor superfamily, member 11b (osteoprotegerin)	0.04816	2.390
205901_at	PNOC	prepronociceptin	0.04851	4.542
209771_x_at	CD24	CD24 molecule	0.04851	2.509
205524_s_at	HAPLN1	hyaluronan and proteoglycan link protein 1	0.04911	3.479

Supplementary Table S2. List of genes whose expression was significantly up-regulated in OS patients who developed pulmonary metastasis ($P < 0.05$)

Probe Set ID	Gene symbol	Description	*P*-value	Fold change
204160_s_at	ENPP4	ectonucleotide pyrophosphatase/phosphodiesterase 4 (putative function)	0.00894	2.124
227290_at	---	CDNA FLJ13598 fis, clone PLACE1009921	0.01817	2.012
204913_s_at	SOX11	SRY (sex determining region Y)-box 11	0.04052	3.869
206391_at	RARRES1	retinoic acid receptor responder (tazarotene induced) 1	0.04493	2.291
230624_at	SLC25A27	solute carrier family 25, member 27	0.04715	2.111
235183_at	---	CDNA clone IMAGE:5312689	0.04942	3.532

Int. J. Cancer: **125,** 2854–2862 (2009)
© 2009 UICC

Genome-wide DNA methylation profiles in liver tissue at the precancerous stage and in hepatocellular carcinoma

Eri Arai[1], Saori Ushijima[1], Masahiro Gotoh[1], Hidenori Ojima[1], Tomoo Kosuge[2], Fumie Hosoda[3], Tatsuhiro Shibata[3], Tadashi Kondo[4], Sana Yokoi[5], Issei Imoto[5], Johji Inazawa[5], Setsuo Hirohashi[1] and Yae Kanai[1]*

[1]*Pathology Division, National Cancer Center Research Institute, Tokyo, Japan*
[2]*Hepatobiliary and Pancreatic Surgery Division, National Cancer Center Hospital, Tokyo, Japan*
[3]*Cancer Genomics Project, National Cancer Center Research Institute, Tokyo, Japan*
[4]*Proteome Bioinformatics Project, National Cancer Center Research Institute, Tokyo, Japan*
[5]*Department of Molecular Cytogenetics, Medical Research Institute and School of Biomedical Science, Tokyo Medical and Dental University, Tokyo, Japan*

To clarify genome-wide DNA methylation profiles during hepatocarcinogenesis, bacterial artificial chromosome (BAC) array-based methylated CpG island amplification was performed on 126 tissue samples. The average numbers of BAC clones showing DNA hypo- or hypermethylation increased from noncancerous liver tissue obtained from patients with hepatocellular carcinomas (HCCs) (N) to HCCs. N appeared to be at the precancerous stage, showing DNA methylation alterations that were correlated with the future development of HCC. Using Wilcoxon test, 25 BAC clones, whose DNA methylation status was inherited by HCCs from N and were able to discriminate 15 N samples from 10 samples of normal liver tissue obtained from patients without HCCs (C) with 100% sensitivity and specificity, were identified. The criteria using the 25 BAC clones were able to discriminate 24 additional N samples from 26 C samples in the validation set with 95.8% sensitivity and 96.2% specificity. Using Wilcoxon test, 41 BAC clones, whose DNA methylation status was able to discriminate patients who survived more than 4 years after hepatectomy from patients who suffered recurrence within 6 months and died within a year after hepatectomy, were identified. The DNA methylation status of the 41 BAC clones was correlated with the cancer-free and overall survival rates of patients with HCC. Multivariate analysis revealed that satisfying the criteria using the 41 BAC clones was an independent predictor of overall outcome. Genome-wide alterations of DNA methylation may participate in hepatocarcinogenesis from the precancerous stage, and DNA methylation profiling may provide optimal indicators for carcinogenetic risk estimation and prognostication.
© *2009 UICC*

Key words: bacterial artificial chromosome array-based methylated CpG island amplification; hepatocellular carcinoma; multistage carcinogenesis; precancerous condition; prognostication

Alteration of DNA methylation is one of the most consistent epigenetic changes in human cancers.[1,2] It is known that DNA hypomethylation results in chromosomal instability as a result of changes in the chromatin structure, and that DNA hypermethylation of CpG islands silences tumor-related genes in cooperation with histone modification in human cancers.[3,4]

With respect to hepatocarcinogenesis, we have shown that alterations of DNA methylation at multiple chromosomal loci can be detected even in noncancerous liver tissue showing chronic hepatitis or cirrhosis, which are widely considered to be precancerous conditions, but not in normal liver tissue, using classical Southern blotting analysis.[5] This was one of the earliest reports of alterations of DNA methylation at the precancerous stage. Multiple tumor-related genes, such as the *E-cadherin*[6,7] and *hypermethylated-in-cancer (HIC)-1*[8] genes, are silenced by DNA hypermethylation in hepatocellular carcinomas (HCCs). DNA methyltransferase (DNMT) 1 expression is significantly higher even in noncancerous liver tissue showing chronic hepatitis or cirrhosis than in the normal liver tissue and is even higher in HCCs.[9,10] DNMT1 overexpression is also correlated with poorer tumor differentiation, portal vein involvement and intrahepatic metastasis of HCCs and poorer patient outcome.[11] On the other hand, overexpression of DNMT3b4, an inactive splice variant of DNMT3b, may lead to chromosomal instability through induction of DNA hypomethylation in pericentromeric satellite regions during hepatocarcinogenesis.[12]

Because aberrant DNA methylation is one of the earliest molecular events during hepatocarcinogenesis and also participates in malignant progression,[13,14] it may be possible to estimate the future risk of developing more malignant HCCs on the basis of DNA methylation status. However, only a few previous studies focusing on HCCs have used recently developed array-based technology for assessing genome-wide DNA methylation status,[15] and such studies have focused mainly on identification of tumor-related genes that are silenced by DNA methylation. DNA methylation profiles, which could become the optimum indicator for carcinogenetic risk estimation and prediction of patient outcome, should therefore be further explored during hepatocarcinogenesis using array-based approaches.

In this study, to clarify genome-wide DNA methylation profiles during multistage hepatocarcinogenesis, we performed bacterial artificial chromosome (BAC) array-based methylated CpG island amplification (BAMCA)[16–18] using a microarray of 4,361 BAC clones[19] in the normal liver tissue obtained from patients without HCCs, noncancerous liver tissue obtained from patients with HCCs, and in HCCs themselves.

Material and methods

Patients and tissue samples

As a learning cohort, 15 samples of the noncancerous liver tissue (N1 to N15) and 19 primary HCCs (T1 to T19) were obtained from surgically resected specimens from 16 patients who underwent partial hepatectomy at the National Cancer Center Hospital, Tokyo, Japan. The patients comprised 13 men and 3 women with a mean (±SD) age of 64.9 ± 7.4 years. Of these, 7 were positive for hepatitis B virus (HBV) surface antigen (HBs-Ag), 8 were positive for anti-hepatitis C virus (HCV) antibody (anti-HCV) and 1 was negative for both. Histological examination of the noncancerous liver tissue samples revealed findings compatible with chronic hepatitis in 5 and cirrhosis in 9 and no remarkable histological findings in 1.

Additional Supporting Information may be found in the online version of this article.

Grant sponsors: Ministry of Health, Labor and Welfare of Japan (Third Term Comprehensive 10-Year Strategy for Cancer Control and Cancer Research), New Energy and Industrial Technology Development Organization (NEDO), National Institute of Biomedical Innovation (NiBio) (Program for Promotion of Fundamental Studies in Health Sciences).

***Correspondence to:** Pathology Division, National Cancer Center Research Institute, 5-1-1 Tsukiji, Chuo-ku, Tokyo 104-0045, Japan. Fax: +81-3-3248-2463. E-mail: ykanai@ncc.go.jp

Received 3 February 2009; Accepted after revision 25 June 2009
DOI 10.1002/ijc.24708
Published online 30 June 2009 in Wiley InterScience (www.interscience.wiley.com).

For the comparison, 10 normal liver tissue samples (C1 to C10) showing no remarkable histological findings were also obtained from 10 patients without HCCs who were both HBs-Ag- and anti-HCV-negative. The patients comprised 7 men and 3 women with a mean age of 58.4 ± 9.7 years. Nine patients underwent partial hepatectomy for liver metastases of primary colon cancers, and 1 patient did so for liver metastases of gastrointestinal stromal tumor of the stomach.

In addition, for the comparison, 7 liver tissue samples (V1 to V7) were obtained from 7 patients who were positive for HBs-Ag or anti-HCV, but who had never developed HCCs. The patients comprised 4 men and 3 women with a mean age of 62.4 ± 5.2 years. Three patients underwent partial hepatectomy for liver metastases of primary colon or rectal cancers, and 1 patient did so for liver metastases of gastric cancer. Three patients underwent partial hepatectomy for cholangiocellular carcinomas.

As a validation cohort, 26 normal liver tissue samples (C11 to C36) showing no remarkable histological features were obtained from 26 patients without HCCs who were both HBs-Ag- and anti-HCV-negative. Twenty-four noncancerous liver tissue samples (N16 to N 39) and 25 primary HCCs (T20 to T44) were obtained from surgically resected specimens from 24 patients who underwent partial hepatectomy were added. The patients from whom C11 to C36 were obtained comprised 21 men and 5 women with a mean age of 59.9 ± 10.9 years. The patients with HCCs from whom N16 to N 39 and T20 to T44 were obtained comprised 22 men and 2 women with a mean age of 61.6 ± 11.4 years. Of the 24 patients with HCCs from whom N16 to N 39 and T20 to T44 were obtained, 5 were positive for HBs-Ag, 16 were positive for anti-HCV and 3 were negative for both. Histological examination of N16 to N 39 revealed findings compatible with chronic hepatitis and cirrhosis in 16 and 8 samples, respectively.

This study was approved by the Ethics Committee of the National Cancer Center, Tokyo, Japan.

BAMCA

High molecular weight DNA from fresh-frozen tissue samples was extracted using phenol-chloroform followed by dialysis. Because DNA methylation status is known to be organ specific, the reference DNA for analysis of the developmental stages of HCCs should be obtained from the liver and not from other organs or peripheral blood. Therefore, a mixture of normal liver tissue DNA obtained from 5 male patients (C37 to C41) and 5 female patients (C42 to C46) was used as a reference for analyses of male and female test DNA samples, respectively.

DNA methylation status was analyzed by BAMCA using a custom-made array (MCG Whole Genome Array-4500) harboring 4,361 BAC clones located throughout chromosomes 1 to 22 and X and Y,[19] as described previously.[16–18] Briefly, 5-μg aliquots of test or reference DNA were first digested with 100 units of methylation-sensitive restriction enzyme *Sma* I and subsequently with 20 units of methylation-insensitive *Xma* I. Adapters were ligated to *Xma* I-digested sticky ends, and polymerase chain reaction (PCR) was performed with an adapter primer set. Test and reference PCR products were labeled by random priming with Cy3- and Cy5-dCTP (GE Healthcare, Buckinghamshire, UK), respectively, and precipitated together with ethanol in the presence of Cot-I DNA. The mixture was applied to array slides and incubated at 43°C for 72 hr. Arrays were scanned with a GenePix Personal 4100A (Axon Instruments, Foster City, CA) and analyzed using GenePix Pro 5.0 imaging software (Axon Instruments) and Acue 2 software (Mitsui Knowledge Industry, Tokyo, Japan). The signal ratios were normalized in each sample to make the mean signal ratios of all BAC clones 1.0.

Statistics

Differences in the average number of BAC clones that showed DNA methylation alterations between groups of samples were analyzed using the Mann-Whitney *U* test or the Kruskal-Wallis test. Correlations between DNA methylation alterations in noncancerous liver tissue samples and the incidence of metachronous development and recurrence of HCCs were analyzed using the chi-squared test. Differences at $p < 0.05$ were considered significant. BAC clones whose signal ratios yielded by BAMCA were significantly different between groups of samples were identified by Wilcoxon test ($p < 0.01$). A support vector machine algorithm and a leave-one-out cross-validation were used to identify BAC clones by which the cumulative error rate for discrimination of sample groups became minimal. Two-dimensional hierarchical clustering analysis of noncancerous liver tissue samples and the BAC clones, and such analysis of HCCs and the BAC clones, were performed using the Expressionist software program (Gene Data, Basel, Switzerland). Survival curves of patient groups with HCCs were calculated by the Kaplan-Meier method, and the differences were compared by the log-rank test. The Cox proportional hazards multivariate model was used to examine the prognostic impact of DNA methylation status, histological differentiation, portal vein tumor thrombi, intrahepatic metastasis and multicentricity. Differences at $p < 0.05$ were considered significant.

Results

Genome-wide DNA methylation alterations during multistage hepatocarcinogenesis

Figures. 1*a* and 1*b* show examples of scanned array images and scattergrams of the signal ratios (test signal/reference signal), respectively, for normal liver tissue from a patient without HCC (Panel C), and both noncancerous liver tissue (Panel N) and cancerous tissue (Panel T) from a patient with HCC. In all normal liver tissue samples, the signal ratios of 97% of the BAC clones were between 0.67 and 1.5 (red bars in Fig. 1*b*). Therefore, in noncancerous liver tissue obtained from patients with HCCs and HCCs, DNA methylation status corresponding to a signal ratio of less than 0.67 and more than 1.5 was defined as DNA hypomethylation and DNA hypermethylation of each BAC clone compared with normal liver tissue, respectively.

In samples of noncancerous liver tissue obtained from patients with HCCs, many BAC clones showed DNA hypo- or hypermethylation (Panel N of Fig. 1*b*). In the learning cohort, all 9 patients (100%) showing DNA hypo- or hypermethylation on 70 or more than 70 BAC clones in their noncancerous liver tissue samples developed metachronous or recurrent HCCs after hepatectomy, whereas only 2 (30%) of the 6 patients showing DNA hypo- or hypermethylation on less than 70 BAC clones in their noncancerous liver tissue samples did so ($p = 0.0235$).

In HCCs themselves, more BAC clones showed DNA hypo- or hypermethylation, and the degree of DNA hypo- or hypermethylation, *i.e.*, deviation of the signal ratio from 0.67 or 1.5, was increased (Panel T of Fig. 1*b*) in comparison with noncancerous liver tissue obtained from patients with HCCs. The average numbers of BAC clones showing a signal ratio of less than 0.67 ($p = 0.0000063$) and more than 1.5 ($p = 0.00000052$) were increased significantly relative to normal liver tissue, to noncancerous liver tissue obtained from patients with HCCs, and to HCCs (Table I).

There were no significant differences in the number of BAC clones showing DNA hypo- or hypermethylation in samples of normal liver tissue obtained from male and female patients without HCCs (66.0 ± 30.1 and 98.7 ± 55.9, $p = 0.362$) and noncancerous liver tissue (111.2 ± 68.4 and 60.7 ± 46.9, $p = 0.279$) and cancerous tissue (521.5 ± 255.8 and 626.7 ± 329.0, $p = 0.539$) obtained from male and female patients with HCCs, respectively. Although there were no significant differences in the number of BAC clones showing DNA hypo- or hypermethylation between HBV- and HCV-positive patients with HCCs in both noncancerous liver tissue (108.3 ± 80.5 and 98.4 ± 60.0, $p = 1.000$) and cancerous tissue (475.6 ± 323.8 and 497.0 ± 247.8, $p = 0.689$), Wilcoxon test ($p < 0.01$) identified BAC clones in which DNA methylation status differed significantly between HBV- and

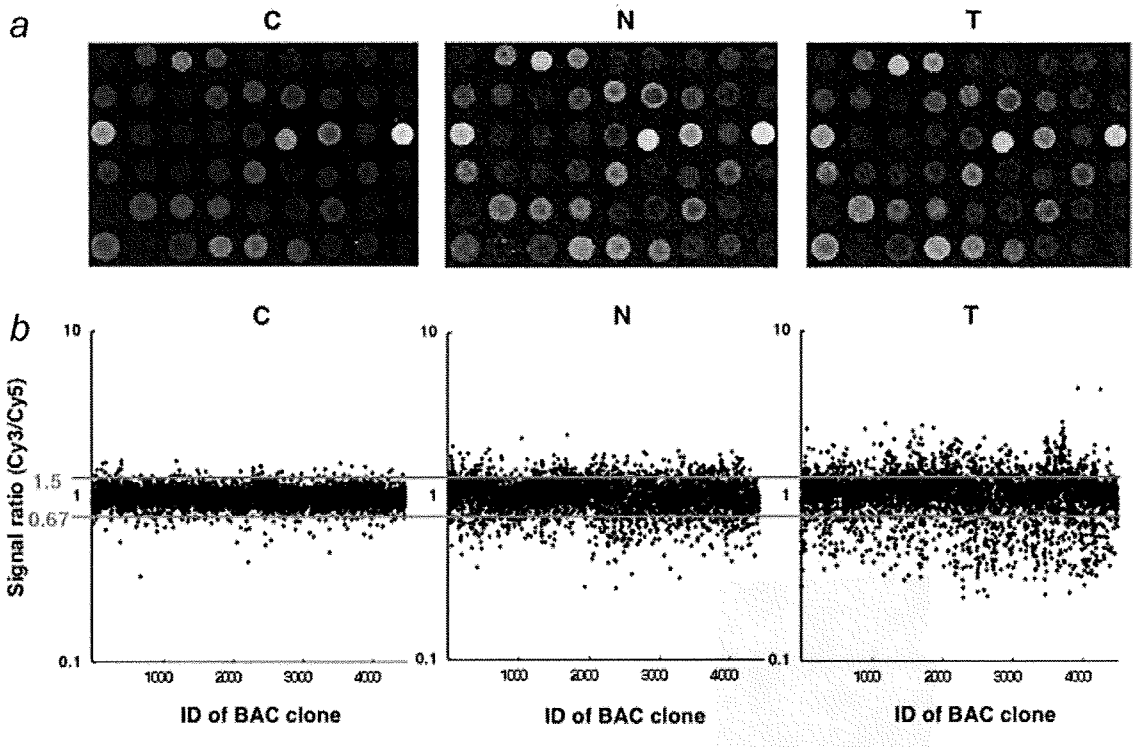

FIGURE 1 – Genome-wide DNA methylation alterations during multistage hepatocarcinogenesis. (*a*) Scanned array images yielded by BAMCA in normal liver tissue obtained from a patient without HCC (C) and noncancerous liver tissue (N) and cancerous tissue (T) obtained from a patient with HCC. (*b*) Scattergrams of the signal ratios yielded by BAMCA. In all C samples, the signal ratios of 97% of BAC clones were between 0.67 and 1.5 (red bars). In N and T, DNA methylation status corresponding to a signal ratio of less than 0.67 and more than 1.5 was defined as DNA hypomethylation and DNA hypermethylation on each BAC clone compared with C, respectively. Even in N, many BAC clones showed DNA hypo- or hypermethylation. In T, more BAC clones showed DNA hypo- or hypermethylation, and the degree of DNA hypo- or hypermethylation, *i.e.*, deviation of the signal ratio from 0.67 or 1.5 was increased in comparison with N.

TABLE I – GENOME-WIDE DNA METHYLATION ALTERATIONS DURING MULTISTAGE HEPATOCARCINOGENESIS

Tissue samples	Average number of BAC clones (mean ± SD)					
	Signal ratio <0.67 (DNA hypomethylation)	*p*	Signal ratio >1.5 (DNA hypermethylation)	*p*	Signal ratio <0.67 or >1.5(DNA hypo- or hypermethylation)	*p*
Normal liver tissue samples obtained from patient without HCCs (C, $n = 10$)	39.9 ± 20.8	0.0000063[1]	38.9 ± 24.9	0.00000052[1]	75.8 ± 39.3	0.00000061[1]
Noncancerous liver tissue samples obtained from patient with HCCs (N, $n = 15$)	61.2 ± 46.8	0.000102[2]	39.9 ± 27.3	0.0000026[2]	101.1 ± 66.5	0.0000065[2]
HCCs (T, $n = 19$)	278.9 ± 167.7	–	228.9 ± 125.7	–	507.8 ± 281.9	–

p values <0.05, which indicate significant differences.
[1]Kruskal-Wallis test among C, N and T.–[2]Mann-Whitney *U* test between N and T.

HCV-positive patients with HCCs in noncancerous liver tissue (18 BAC clones) and cancerous tissue (15 BAC clones), respectively.

DNA methylation profiles discriminating noncancerous liver tissue obtained from patients with HCCs from normal liver tissue

The above findings indicating accumulation of clinicopathologically significant genome-wide DNA methylation alterations in noncancerous liver tissue prompted us to estimate the degree of carcinogenetic risk based on DNA methylation profiles. Wilcoxon test ($p < 0.01$) revealed that the signal ratios of 512 BAC clones differed significantly between normal liver tissue samples and noncancerous liver tissue samples obtained from patients with HCCs. To omit potentially insignificant BAC clones associated only with inflammation and/or fibrosis and focus on BAC clones for which DNA methylation status was inherited by HCCs from the precancerous stage, we defined Groups I, II, III and IV. Group I: BAC clones in which the average signal ratio of noncancerous liver tissue obtained from patients with HCCs was higher than that of normal liver tissue and the average signal ratio of HCCs was even higher than that of noncancerous liver tissue obtained from patients with HCCs (41 BAC clones), Group II: BAC clones in which the average signal ratio of noncancerous liver tissue obtained from patients with HCCs was higher than that of normal liver tissue and the average signal ratio of HCCs did not differ from that of noncancerous liver tissue obtained from patients with HCCs (146 BAC clones), Group III: BAC clones in which the average signal ratio of noncancerous liver tissue obtained from patients with HCCs was lower than that of normal liver tissue and the average signal ratio of HCCs was even lower than that of noncancerous liver tissue obtained from patients with HCCs (40 BAC clones), and Group IV: BAC clones in which the average signal ratio of noncancerous liver tissue obtained from patients with HCCs was lower than that of normal liver tissue and the average

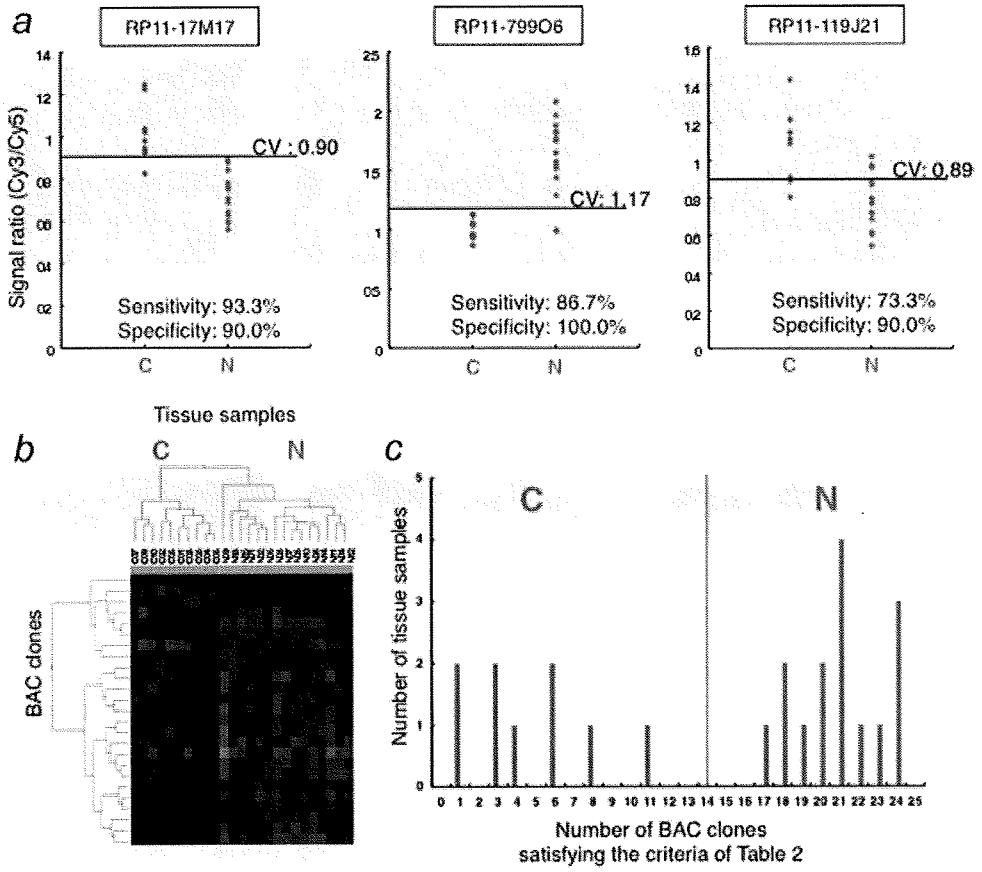

FIGURE 2 – DNA methylation profiles discriminating noncancerous liver tissue obtained from patients with HCCs from normal liver tissue. (*a*) Scattergrams of the signal ratios in normal liver tissue samples (C1 to C10) and noncancerous liver tissue samples obtained from patients with HCCs (N1 to N15) in the learning cohort on representative BAC clones, RP11-17M17, RP11-799O6 and RP11-119J21. Using the cutoff values (CV) described in each panel, noncancerous liver tissue samples obtained from patients with HCCs (N) in the learning cohort were discriminated from normal liver tissue samples (C) with sufficient sensitivity and specificity. (*b*) By 2-dimensional hierarchical clustering analysis using the 25 BAC clones selected by the process described in the Results section, normal liver tissue samples (C1 to C10) and noncancerous liver tissue samples obtained from patients with HCCs (N1 to N15) in the learning cohort were subclassified into the different subclasses without any error. The cluster trees for tissue samples and BAC clones are shown at the top and left of the panel, respectively. (*c*) Histogram showing the number of BAC clones satisfying the Table II criteria in samples C1 to C10 and N1 to N15. On the basis of this histogram, we established the following criteria: when the noncancerous liver tissue satisfied the criteria in Table II for 14 (green bar) or more than 14 BAC clones, it was judged to be at high risk of carcinogenesis.

signal ratio of HCCs did not differ from that of noncancerous liver tissue obtained from patients with HCCs (131 BAC clones). From the 512 BAC clones, 358 (Groups I, II, III and IV), in which the DNA methylation status was inherited by HCCs from noncancerous liver tissue, were selected. From the 358 BAC clones, the first 40 were identified by spot ranking analysis using the support vector machine algorithm for discrimination of noncancerous liver tissue obtained from patients with HCCs from normal liver tissue. Figure 2*a* shows scattergrams of the signal ratios in normal liver tissue samples and noncancerous liver tissue samples obtained from patients with HCCs on representative examples of the 40 BAC clones. Using the cutoff values described in each panel, noncancerous liver tissue obtained from patients with HCCs in the learning cohort was discriminated from normal liver tissue with sufficient sensitivity and specificity (Fig. 2*a*). From the 40 BAC clones, 25, for which such discrimination was performed with a sensitivity or specificity of 70% or more than 70%, were selected (Supporting Information Table S1). The cutoff values of the signal ratios for the 25 BAC clones, and their sensitivity and specificity, are shown in Table II. Two-dimensional hierarchical clustering analysis using the 25 BAC clones is shown in Figure 2*b*: 10 normal liver tissue samples (C1 to C10) and 15 noncancerous liver tissue samples obtained from patients with HCCs (N1 to N15) in the learning cohort were subclassified into different subclasses without any error. The number of BAC clones satisfying the criteria listed in Table II in noncancerous liver tissue samples showing chronic hepatitis (20.6 ± 1.8) was not significantly different from that showing cirrhosis (21.3 ± 2.4, $p = 0.542$) in the learning cohort.

A histogram showing the number of BAC clones satisfying the criteria listed in Table II for samples C1 to C10 and N1 to N15 is shown in Figure 2*c*. On the basis of this figure, we finally established the following criteria: when noncancerous liver tissue satisfied the criteria of Table II for 14 or more BAC clones (green bar in Fig. 2*c*), it was judged to be at high risk of carcinogenesis, and when noncancerous liver tissue satisfied the criteria of Table II for less than 14 BAC clones, it was judged not to be at high risk of carcinogenesis. Based on these criteria, both the sensitivity and specificity for diagnosis of noncancerous liver tissue samples obtained from patients with HCCs in the learning cohort as being at high risk of carcinogenesis were 100%.

To confirm these criteria, an additional 50 liver tissue samples were analyzed by BAMCA as a validation study (Supporting Information Figure S1). Twenty-three of 24 validation samples satisfying the criteria of Table II for 14 or more BAC clones were noncancerous liver tissue samples obtained from patients with HCCs (N16 to N36 and N38), and 24 of 26 validation samples satisfying the criteria of Table II for less than 14 BAC clones were normal

TABLE II – 25 BAC CLONES WHICH COULD DISCRIMINATE NONCANCEROUS LIVER TISSUES (N) FROM NORMAL LIVER TISSUES (C)

BAC clone ID	Location	Cutoff value	DNA methylation status[1]	Sensitivity (%)	Specificity (%)
RP11-104J13	1p35-1p36	1.01	C>N	93.3	70.0
RP11-52I2	1p34-1p35	1.00	C<N	80.0	60.0
RP11-29M22	1p11-1p12	1.11	C<N	86.7	90.0
RP11-21K1	2q37.2	1.00	C>N	86.7	70.0
RP11-109B15	5q33	1.04	C<N	66.7	90.0
RP11-88B24	6q26	0.95	C>N	80.0	70.0
RP11-112B7	7p13-7p14	1.00	C>N	80.0	70.0
RP11-48D21	8p11.2	1.00	C>N	80.0	90.0
RP11-120E20	11p15.4-11p15.5	0.90	C>N	73.3	100.0
RP11-334E6	11q23	1.00	C>N	86.7	80.0
RP11-17M17	11q25	0.90	C>N	93.3	90.0
RP11-319E16	12p13.32a	1.00	C>N	80.0	90.0
RP11-1100L3	12q13.13c-12q13.13d	1.04	C<N	86.7	80.0
RP11-799O6	12q13.3a-12q13.3b	1.17	C<N	86.7	100.0
RP11-119J21	12q24.33	0.89	C>N	73.3	90.0
RP11-332N6	14q11.2b	0.95	C>N	86.7	100.0
RP11-529E4	14q12c	1.00	C>N	93.3	50.0
RP11-89M4	16p13.2-16p13.3	1.20	C<N	86.7	100.0
RP11-215M5	15q15-15q21.1	1.00	C<N	86.7	70.0
RP11-348B12	19p13	1.00	C<N	80.0	80.0
RP11-134G22	20p11.2-20p12	1.01	C>N	80.0	90.0
RP11-328M17	22q13.2-22q13.33	0.93	C>N	86.7	100.0
RP11-354I12	22q13.31-22q13.33	1.00	C>N	93.3	80.0
RP11-55J11	22q13.2-22q13.33	1.00	C>N	80.0	70.0
RP11-480M11	Xq27.1-Xq28	0.90	C>N	80.0	90.0

[1]C>N, when the signal ratio was lower than the cutoff value, the tissue sample was considered to be at high risk for carcinogenesis; C<N, when the signal ratio was higher than the cutoff value, the tissue sample was considered to be at high risk for carcinogenesis.

liver tissue samples (C11 to C31, 33, 34 and 36). That is, our criteria enabled diagnosis of noncancerous liver tissue samples obtained from patients with HCCs in the validation set as being at high risk of carcinogenesis with a sensitivity of 95.8% and a specificity of 96.2%. The number of BAC clones satisfying the criteria listed in Table II in noncancerous liver tissue samples showing chronic hepatitis (17.6 ± 2.5) was not significantly different from that showing cirrhosis (19.4 ± 1.8, $p = 0.128$) in the validation cohort.

In addition, the average number of BAC clones satisfying the criteria in Table II was significantly lower in 7 samples of liver tissue obtained from patients who were infected with HBV or HCV, but who had never developed HCCs (V1 to V7, 13.14 ± 4.78), than that in N1 to N39 (19.21 ± 2.67, $p = 0.00419$).

Association of HCC DNA methylation profiles with patient outcome

To establish criteria for prognostication of patients with HCCs, in the learning cohort, 5 of 19 HCC samples obtained from patients who had survived more than 4 years after hepatectomy and 6 of 19 HCC samples from patients who had suffered recurrence within 6 months and died within a year after hepatectomy were defined as a favorable-outcome group and a poor-outcome group, respectively. Wilcoxon test ($p < 0.01$) revealed that the signal ratios of 41 BAC clones (Supporting Information Table S1) differed significantly between the favorable-outcome group ($n = 5$) and the poor-outcome group ($n = 6$). Figure 3*a* shows scattergrams of the signal ratios in samples from the favorable- and poor-outcome groups for representative examples of the 41 BAC clones. Using the cutoff values described in Figure 3*a* and Table III for the 41 BAC clones, samples from the poor-outcome group were discriminated from favorable-outcome group samples with sufficient sensitivity and specificity (Fig. 3*a* and Table III). Two-dimensional hierarchical clustering analysis using the 41 BAC clones is shown in Figure 3*b*: 5 HCCs in the favorable-outcome group and 6 HCCs in the poor-outcome group were subclassified into different subclasses without any error (Fig. 3*b*). A histogram showing the number of BAC clones satisfying the criteria in Table III is shown in Fig. 3*c*. In all 19 HCCs in the learning cohort, multivariate analysis revealed that satisfying the criteria in Table III for 32 or more BAC clones was a predictor of overall patient outcome and was independent of parameters that are already known to have prognostic impact,[20] such as histological differentiation, portal vein tumor thrombi, intrahepatic metastasis and multicentricity (Table IV).

To confirm these criteria, an additional 25 HCC samples were analyzed by BAMCA as a validation study, and then evaluated based on the criteria in Table III. All 44 HCCs were divided into 2 groups according to the number of BAC clones satisfying the criteria (32 or more BAC clones *vs.* less than 32 BAC clones). The period covered ranged from 11 to 3,413 days (mean, 1,349 days). The cancer-free and overall survival rates of patients with HCCs satisfying the criteria in Table III for 32 or more BAC clones was significantly lower than that of patients with HCCs satisfying the criteria in Table III for less than 32 BAC clones (Fig. 3*d*, $p = 0.000000002$ and $p = 0.0013$, respectively).

Discussion

Although many researchers in the field of cancer epigenetics use promoter arrays to identify the genes that are methylated in cancer cells,[21–23] we used a BAC array[19] in this study. The efficiency of identification of specific genes that are silenced by DNA methylations around the promoter regions and may become a target of therapy may be generally lower using the BAMCA approach than with conventional promoter array-based analysis. However, the promoter regions of specific genes are not the only target of DNA methylation alterations in human cancers. DNA methylation status in genomic regions not directly participating in gene silencing, such as the edges of CpG islands, may be altered at the precancerous stage before the alterations of the promoter regions themselves occur.[24] Moreover, aberrant DNA methylation of large regions of chromosomes, which are regulated in a coordinated manner in human cancers due to a process of long-range epigenetic silencing, has recently attracted attention.[25] BAMCA methods may be suitable for overviewing the DNA methylation status of individual large regions among all chromosomes and for

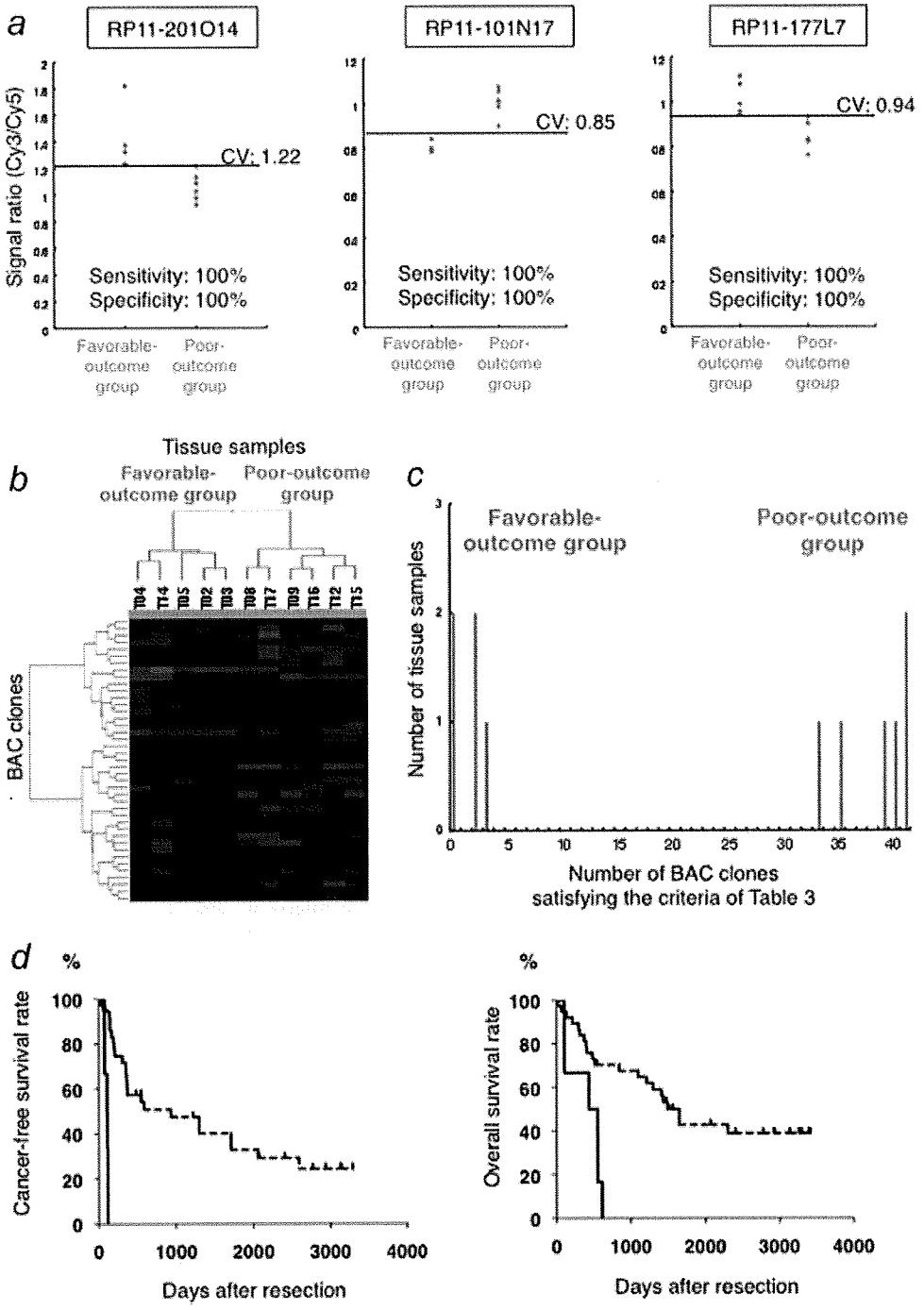

FIGURE 3 – DNA methylation profiles in HCCs associated with patient outcome. (*a*) Scattergrams of the signal ratios in HCCs from patients who survived more than 4 years after hepatectomy (favorable-outcome group, $n = 5$) and HCCs from patients who suffered recurrence within 6 months and died within a year after hepatectomy (poor-outcome group, $n = 6$) in the learning cohort for representative BAC clones, RP11-201O14, RP11-101N17 and RP11-177L7. Using the described cutoff values (CV), the poor-outcome group was discriminated from the favorable-outcome group with 100% sensitivity and specificity. (*b*) By 2-dimensional hierarchical clustering analysis using the 41 BAC clones selected by Wilcoxon test, HCCs in the favorable-outcome group and those in the poor-outcome group in the learning cohort were subclassified in the different subclasses without any error. The cluster trees for tissue samples and BAC clones are shown at the top and left of the panel, respectively. (*c*) Histogram showing the number of BAC clones satisfying the Table III criteria in HCCs of the favorable- and poor-outcome groups in the learning cohort. (*d*) Kaplan-Meier survival curves of all patients with HCCs (T1 to T44). The cancer-free (left panel, $p = 0.000000002$) and overall (right panel, $p = 0.0013$) survival rates of patients with HCCs satisfying the Table III criteria for 32 or more than 32 BAC clones (solid lines) were significantly lower than that of patients with HCCs satisfying the Table III criteria for less than 32 BAC clones (broken lines).

TABLE III – 41 BAC CLONES WHICH COULD DISCRIMINATE HCCS IN POOR-OUTCOME GROUP (P) FROM THOSE IN FAVORABLE-OUTCOME GROUP (F)

BAC clone ID	Location	Cutoff value	DNA methylation status[1]	Sensitivity (%)	Specificity (%)
RP11-89K16	1p35	1.50	F<P	83.3	100.0
RP11-201O14	1p34.3-1p36.13	1.22	F>P	100.0	100.0
RP11-156K6	1p31.1-1p31.3	1.15	F>P	100.0	80.0
RP11-553K8	1q31.2-1q31.3	1.16	F>P	100.0	100.0
RP11-89E10	1q31.3	0.91	F<P	100.0	100.0
RP11-180L21	2p16-2p21	1.29	F>P	100.0	80.0
RP11-90B13	2p14-2p15	1.13	F>P	83.3	100.0
RP11-449B19	2q11.2	0.75	F<P	100.0	80.0
RP11-30M1	2q32.3	1.10	F<P	100.0	100.0
RP11-89B13	2q32.3-2q33.1	1.11	F>P	83.3	80.0
RP11-255O19	3p24.3-3p25	1.08	F>P	100.0	100.0
RP11-421F9	3p24.2a	0.97	F>P	83.3	100.0
RP11-122D19	3p21.2	0.99	F<P	100.0	80.0
RP11-36K8	4q22	0.91	F>P	83.3	100.0
RP11-101N17	4q26	0.85	F<P	100.0	100.0
RP11-177L7	4q32	0.94	F>P	100.0	100.0
RP11-13O14	4q34-4q35	0.88	F<P	83.3	100.0
RP11-88H16	5p14	0.85	F<P	100.0	100.0
RP11-91G9	5q22-5q23	1.45	F<P	83.3	100.0
RP11-79K22	6q16	0.98	F<P	83.3	100.0
RP11-126B8	7q21.3	1.06	F>P	100.0	100.0
RP11-89P11	7q35	0.83	F>P	83.3	100.0
RP11-88N8	8q21.11d	1.02	F>P	100.0	100.0
RP11-85C21	9q33.3-9q34.2	0.95	F<P	83.3	100.0
RP11-714M16	10q26.11-10q26.3	1.00	F<P	100.0	100.0
RP11-48A2	10q26.2	0.69	F<P	100.0	80.0
RP11-206I1	11p11.2	1.20	F<P	100.0	100.0
RP11-35F11	11q12	1.30	F<P	100.0	80.0
RP11-158I9	11q23	1.04	F>P	83.3	100.0
RP11-74I8	12q13	1.13	F<P	100.0	100.0
RP11-167B4	16p13.3	0.97	F>P	83.3	100.0
RP11-368N21	16p11.2-16p12	1.10	F>P	83.3	100.0
RP11-303G21	16q12.1b	0.80	F>P	83.3	100.0
RP11-151M19	16q22	1.05	F>P	100.0	100.0
RP11-135N5	17p13.2	1.00	F>P	100.0	100.0
RP11-398A1	17q11.2d	1.00	F>P	100.0	100.0
RP11-15A1	19q13	1.08	F>P	83.3	100.0
RP11-697B10	19q13.3	0.90	F>P	83.3	100.0
RP11-79A3	19q13.3	1.05	F<P	100.0	100.0
RP11-29H19	20q12	1.00	F>P	100.0	100.0
RP11-36N5	22q11.2	1.15	F>P	83.3	100.0

[1]F>P, when the signal ratio was lower than the cutoff value, the tissue sample was considered to have been obtained from a patient with poor prognosis; F<P, when the signal ratio was higher than the cutoff value, the tissue sample was considered to have been obtained from a patient with poor prognosis.

identifying reproducible indicators for carcinogenetic risk estimation and prognostication. In fact, we have successfully obtained optimal indicators for carcinogenetic risk estimation and prognostication of renal cell carcinomas[26] and urothelial carcinomas (data will be published elsewhere) by BAMCA using the same array as that used in this study.

Our previous studies indicated that alterations of DNA methylation are one of the earliest events of multistage hepatocarcinogenesis and participate in malignant progression of HCCs.[5,7-14,27-29] However, since in previous studies we examined DNA methylation status on only a restricted number of CpG islands or chromosomal loci, it has not yet been clarified whether DNA methylation status on only restricted regions is simply altered at the precancerous stage, or whether genome-wide alterations of DNA methylation status have certain clinicopathological significance. As shown in Panel N of Figure 1*b*, genome-wide DNA methylation alterations (both hypo- and hypermethylation) were confirmed even in noncancerous liver tissue samples obtained from patients with HCCs. The number of BAC clones showing DNA methylation alterations and the degree of DNA methylation alterations were found to increase stepwise from the precancerous stage to the HCC stage (Fig. 1*b* and Table I). This study revealed that alterations of DNA methylation during multistage hepatocarcinogenesis occur in a genome-wide manner. Genome-wide DNA methylation alterations may participate in multistage hepatocarcinogenesis potentially through the induction of chromosomal instability and silencing of tumor-suppressor genes. DNA methylation alterations in noncancerous liver tissue were correlated with the future development of HCCs, suggesting that DNA methylation alterations at the precancerous stage may not occur randomly but are prone to further accumulation of genetic and epigenetic alterations.

Although mass vaccination against HBV has been initiated, this will not have a major impact for many years, as the age at presentation of HBV is older than 50 years mainly in Asia and Africa.[30] The spread of HCV in Japan that occurred in the 1950s and 1960s has resulted in a rapid increase in the incidence of HCC since 1980. In other countries including the United States, where HCV infection spread more recently, an increase in the incidence of HCC is imminent.[31] Although there were no significant differences in the number of BAC clones showing DNA hypo- or hypermethylation between HBV- and HCV-positive patients with HCCs, Wilcoxon test identified BAC clones in which DNA methylation status differed significantly between HBV- and HCV-positive patients with HCCs in both noncancerous liver tissue and cancerous tissue, suggesting that the HBV-related carcinogenetic

TABLE IV – MULTIVARIATE ANALYSIS OF CLINICOPATHOLOGICAL PARAMETERS AND DNA METHYLATION PROFILES ASSOCIATED WITH OVERALL OUTCOME IN PATIENTS WITH HCCS

Parameters	Hazard ratio (95% CI)	χ^2	p
Histological differentiation			
Well differentiated	1 (Reference)	0.031	0.8594
Moderately or poorly differentiated	0.817 (0.088-7.616)		
Portal vein tumor thrombi			
Negative	1 (Reference)	2.095	0.1478
Positive	4.474 (0.588-34.033)		
Intrahepatic metastasis[1]			
Negative	1 (Reference)	0.090	0.7647
Positive	1.248 (0.292-5.336)		
Multicentricity[1]			
Negative	1 (Reference)	1.499	0.2209
Positive	0.328 (0.055-1.955)		
The criteria of Table 3			
Satisfying for less than 32 BAC clones	1 (Reference)	4.997	0.0254
Satisfying for 32 or more BAC clones	4.466 (1.202-16.585)		

CI, confidence interval.
[1]In patients with multiple lesions, whether the lesions other than the main tumor from which tissue samples were obtained for this study were intrahepatic metastases of the main tumor or second primary lesions was judged by microscopic observation of hepatectomy specimens based on the previously described criteria.[35]

pathway may result in distinct DNA methylation profiles. These findings are in accordance with a previous report showing that HBV-related proteins can induce DNA methylation alterations.[32]

The effectiveness of surgical resection for HCC is limited, unless the disease is diagnosed early at the asymptomatic stage. Therefore, surveillance at the precancerous stage will become a priority. To reveal the baseline liver histology, microscopic examination of liver biopsy specimens is performed in patients with HBV or HCV infection prior to interferon therapy.[33,34] Therefore, carcinogenetic risk estimation using such liver biopsy specimens will be advantageous for close follow-up of patients who are at high risk of HCC development. Because even subtle alterations of DNA methylation profiles at the precancerous stage are stably preserved on DNA double strands by covalent bonds, they may be better indicators for risk estimation than mRNA and protein expression profiles that can be easily affected by the microenvironment of precursor cells.

The present genome-wide analysis revealed DNA methylation profiles that were able to discriminate noncancerous liver tissue obtained from patients with HCCs from normal liver tissue and diagnose it at high risk of HCC development in the learning set. The sensitivity and specificity in the validation set were 95.8 and 96.2%, respectively, and the criteria listed in Table II were validated. For carcinogenetic risk estimation using liver biopsy specimens obtained prior to interferon therapy, DNA methylation profiles actually associated with carcinogenesis should be discriminated from those associated with inflammation and/or fibrosis. Therefore, we first omitted potentially insignificant BAC clones associated only with inflammation and/or fibrosis and focused on BAC clones for which DNA methylation status was inherited by HCCs from the precancerous stage (Groups I, II, III and IV). In fact, it was confirmed that there were no significant differences in the number of BAC clones satisfying the criteria in Table II between noncancerous liver tissue samples showing chronic hepatitis and noncancerous liver tissue samples showing cirrhosis, not only in the learning set ($p = 0.542$) but also in the validation set ($p = 0.128$), indicating that our criteria were not associated with the degree of inflammation or fibrosis. In addition, the average numbers of BAC clones satisfying the criteria in Table II were significantly lower in liver tissue of patients without HCCs (V1 to V7) than in noncancerous liver tissue of patients with HCCs (N1 to N39), even though the patients from whom V1 to V7 were obtained were infected with HBV or HCV. Therefore, our criteria not only discriminate noncancerous liver tissue obtained from patients with HCCs from normal liver tissue but may also be applicable for classifying liver tissue obtained from patients who are followed up because of HBV or HCV infection, chronic hepatitis or cirrhosis into that which may generate HCCs and that which will not. Our criteria are applicable to both patients with chronic hepatitis and liver cirrhosis, although liver cirrhosis is known to show a more pronounced tendency to lead to HCC development than chronic hepatitis.[20] We intend to validate the reliability of such risk estimation prospectively using liver biopsy specimens obtained prior to interferon therapy from a large cohort of patients. On the basis of the present data, we now consider it justifiable to propose that clinicians can apply a portion of biopsy cores for this type of prospective study.

Because a sufficient quantity of good-quality DNA can be obtained from liver biopsy specimens, PCR-based analyses focusing on individual CpG sites are not always required. Although cut-off values should be modified for widely available standardized reference DNA, array-based analysis that overviews aberrant DNA methylation in each BAC region is immediately applicable to routine laboratory examinations. Moreover, because DNA methylation status of CpG sites is often regulated in a coordinated manner in each individual large region on chromosomes,[13,14,25] an overview of the DNA methylation tendency (hypo- or hypermethylation) in the whole BAC region can be a more reproducible diagnostic indicator than one focusing on individual CpG sites.

The present genome-wide analysis revealed DNA methylation profiles that were able to discriminate a poor-outcome group from a favorable-outcome group. Correlation between the DNA methylation profiles and both cancer-free and overall survival rates of patients with HCCs (Fig. 3*d*) validated the criteria in Table III. Prognostication based on our criteria may be promising for supportive use during follow-up after surgical resection, because multivariate analysis revealed that our criteria can predict overall patient outcome independently of parameters observed in hepatectomy specimens that are already known to have prognostic impact.[20] Such prognostication using liver biopsy specimens obtained before transarterial embolization, transarterial chemoembolization and radiofrequency ablation may be advantageous even to patients who undergo such therapies. The reliability of such prognostication needs to be validated again prospectively in surgically resected specimens or biopsy specimens.

References

1. Jones PA, Baylin SB. The fundamental role of epigenetic events in cancer. Nat Rev Genet 2002;3:415–28.
2. Gronbaek K, Hother C, Jones PA. Epigenetic changes in cancer. APMIS 2007;115:1039–59.
3. Eden A, Gaudet F, Waghmare A, Jaenisch R. Chromosomal instability and tumors promoted by DNA hypomethylation. Science 2003; 300:455.
4. Baylin SB, Ohm JE. Epigenetic gene silencing in cancer—a mechanism for early oncogenic pathway addiction? Nat Rev Cancer 2006;6:107–16.
5. Kanai Y, Ushijima S, Tsuda H, Sakamoto M, Sugimura T, Hirohashi S. Aberrant DNA methylation on chromosome 16 is an early event in hepatocarcinogenesis. Jpn J Cancer Res 1996;87: 1210–7.
6. Yoshiura K, Kanai Y, Ochiai A, Shimoyama Y, Sugimura T, Hirohashi S. Silencing of the E-cadherin invasion-suppressor gene by CpG methylation in human carcinomas. Proc Natl Acad Sci USA 1995;92:7416–9.
7. Kanai Y, Ushijima S, Hui AM, Ochiai A, Tsuda H, Sakamoto M, Hirohashi S. The E-cadherin gene is silenced by CpG methylation in human hepatocellular carcinomas. Int J Cancer 1997; 71:355–9.
8. Kanai Y, Hui AM, Sun L, Ushijima S, Sakamoto M, Tsuda H, Hirohashi S. DNA hypermethylation at the D17S5 locus and reduced HIC-1

mRNA expression are associated with hepatocarcinogenesis. Hepatology 1999;29:703–9.
9. Sun L, Hui AM, Kanai Y, Sakamoto M, Hirohashi S. Increased DNA methyltransferase expression is associated with an early stage of human hepatocarcinogenesis. Jpn J Cancer Res 1997;88:1165–70.
10. Saito Y, Kanai Y, Sakamoto M, Saito H, Ishii H, Hirohashi S. Expression of mRNA for DNA methyltransferases and methyl-CpG-binding proteins and DNA methylation status on CpG islands and pericentromeric satellite regions during human hepatocarcinogenesis. Hepatology 2001;33:561–8.
11. Saito Y, Kanai Y, Nakagawa T, Sakamoto M, Saito H, Ishii H, Hirohashi S. Increased protein expression of DNA methyltransferase (DNMT) 1 is significantly correlated with the malignant potential and poor prognosis of human hepatocellular carcinomas. Int J Cancer 2003;105:527–32.
12. Saito Y, Kanai Y, Sakamoto M, Saito H, Ishii H, Hirohashi S. Overexpression of a splice variant of DNA methyltransferase 3b. DNMT3b4, associated with DNA hypomethylation on pericentromeric satellite regions during human hepatocarcinogenesis. Proc Natl Acad Sci USA 2002;99:10060–5.
13. Kanai Y, Hirohashi S. Alterations of DNA methylation associated with abnormalities of DNA methyltransferases in human cancers during transition from a precancerous to a malignant state. Carcinogenesis 2007;28:2434–42.
14. Kanai Y. Alterations of DNA methylation and clinicopathological diversity of human cancers. Pathol Int 2008;58:544–58.
15. Gao W, Kondo Y, Shen L, Shimizu Y, Sano T, Yamao K, Natsume A, Goto Y, Ito M, Murakami H, Osada H, Zhang J, et al. Variable DNA methylation patterns associated with progression of disease in hepatocellular carcinomas. Carcinogenesis 2008; 29:1901–10.
16. Misawa A, Inoue J, Sugino Y, Hosoi H, Sugimoto T, Hosoda F, Ohki M, Imoto I, Inazawa J. Methylation-associated silencing of the nuclear receptor 1I2 gene in advanced-type neuroblastomas, identified by bacterial artificial chromosome array-based methylated CpG island amplification. Cancer Res 2005;65:10233–42.
17. Sugino Y, Misawa A, Inoue J, Kitagawa M, Hosoi H, Sugimoto T, Imoto I, Inazawa J. Epigenetic silencing of prostaglandin E receptor 2 (PTGER2) is associated with progression of neuroblastomas. Oncogene 2007;26:7401–13.
18. Tanaka K, Imoto I, Inoue J, Kozaki K, Tsuda H, Shimada Y, Aiko S, Yoshizumi Y, Iwai T, Kawano T, Inazawa J. Frequent methylation-associated silencing of a candidate tumor-suppressor. CRABP1, in esophageal squamous-cell carcinoma. Oncogene 2007;26:6456–68.
19. Inazawa J, Inoue J, Imoto I. Comparative genomic hybridization (CGH)-arrays pave the way for identification of novel cancer-related genes. Cancer Sci 2004;95:559–63.
20. Hirohashi S, Ishak KG, Kojiro M, Wanless IR, These ND, Tsukuma H, Blum HE, Deugnier Y, Puig PL, Fischer HP, Sakamoto M. Hepatocellular carcinoma. In: Hamilton SR, Altonen LA, eds. World Health Organization classification of tumours. Pathology and genetics. Tumours of the digestive system. Lyon: IARC Press, 2000. 159–72.
21. Estecio MR, Yan PS, Ibrahim AE, Tellez CS, Shen L, Huang TH, Issa JP. High-throughput methylation profiling by MCA coupled to CpG island microarray. Genome Res 2007;17:1529–36.
22. Jacinto FV, Ballestar E, Ropero S, Esteller M. Discovery of epigenetically silenced genes by methylated DNA immunoprecipitation in colon cancer cells. Cancer Res 2007;67:11481–6.
23. Nielander I, Bug S, Richter J, Giefing M, Martin-Subero JI, Siebert R. Combining array-based approaches for the identification of candidate tumor suppressor loci in mature lymphoid neoplasms. APMIS 2007;115:1107–34.
24. Maekita T, Nakazawa K, Mihara M, Nakajima T, Yanaoka K, Iguchi M, Arii K, Kaneda A, Tsukamoto T, Tatematsu M, Tamura G, Saito D, et al. High levels of aberrant DNA methylation in *Helicobacter pylori*-infected gastric mucosae and its possible association with gastric cancer risk. Clin Cancer Res 2006;12:989–95.
25. Frigola J, Song J, Stirzaker C, Hinshelwood RA, Peinado MA, Clark SJ. Epigenetic remodeling in colorectal cancer results in coordinate gene suppression across an entire chromosome band. Nat Genet 2006; 38:540–9.
26. Arai E, Ushijima S, Fujimoto H, Hosoda F, Shibata T, Kondo T, Yokoi S, Imoto I, Inazawa J, Hirohashi S, Kanai Y. Genome-wide DNA methylation profiles in both precancerous conditions and clear cell renal cell carcinomas are correlated with malignant potential and patient outcome. Carcinogenesis 2009;30:214–21.
27. Kanai Y, Ushijima S, Tsuda H, Sakamoto M, Hirohashi S. Aberrant DNA methylation precedes loss of heterozygosity on chromosome 16 in chronic hepatitis and liver cirrhosis. Cancer Lett 2000;148:73–80.
28. Kondo Y, Kanai Y, Sakamoto M, Mizokami M, Ueda R, Hirohashi S. Genetic instability and aberrant DNA methylation in chronic hepatitis and cirrhosis—A comprehensive study of loss of heterozygosity and microsatellite instability at 39 loci and DNA hypermethylation on 8 CpG islands in microdissected specimens from patients with hepatocellular carcinoma. Hepatology 2000;32:970–9.
29. Kanai Y, Saito Y, Ushijima S, Hirohashi S. Alterations in gene expression associated with the overexpression of a splice variant of DNA methyltransferase 3b, DNMT3b4, during human hepatocarcinogenesis. J Cancer Res Clin Oncol 2004;130:636–44.
30. Chang MH, Chen CJ, Lai MS, Hsu HM, Wu TC, Kong MS, Liang DC, Shau WY, Chen DS. Universal hepatitis B vaccination in Taiwan and the incidence of hepatocellular carcinoma in children. Taiwan Childhood Hepatoma Study Group. N Engl J Med 1997;336:1855–9.
31. Tanaka Y, Hanada K, Mizokami M, Yeo AE, Shih JW, Gojobori T, Alter HJ. Inaugural article: a comparison of the molecular clock of hepatitis C virus in the United States and Japan predicts that hepatocellular carcinoma incidence in the United States will increase over the next two decades. Proc Natl Acad Sci USA 2002;99:15584–9.
32. Park IY, Sohn BH, Yu E, Suh DJ, Chung YH, Lee JH, Surzycki SJ, Lee YI. Aberrant epigenetic modifications in hepatocarcinogenesis induced by hepatitis B virus X protein. Gastroenterology 2007; 132:1476–94.
33. Arase Y, Ikeda K, Suzuki F, Suzuki Y, Kobayashi M, Akuta N, Hosaka T, Sezaki H, Yatsuji H, Kawamura Y, Kobayashi M, Kumada H. Comparison of interferon and lamivudine treatment in Japanese patients with HBeAg positive chronic hepatitis B. J Med Virol 2007; 79:1286–92.
34. Yoshida H, Tateishi R, Arakawa Y, Sata M, Fujiyama S, Nishiguchi S, Ishibashi H, Yamada G, Yokosuka O, Shiratori Y, Omata M. Benefit of interferon therapy in hepatocellular carcinoma prevention for individual patients with chronic hepatitis C. Gut 2004;53:425–30.
35. Oikawa T, Ojima H, Yamasaki S, Takayama T, Hirohashi S, Sakamoto M. Multistep and multicentric development of hepatocellular carcinoma: histological analysis of 980 resected nodules. J Hepatol 2005;42:225–9.